MEASURED FAST-NEUTRON ALBEDOS FOR CONCRETE AND STEEL: COMPARISON WITH CALCULATIONS

by

JOHN WAYNE LEIGHTY

B.S., Kansas State University, 1970

A MASTER'S THESIS

submitted in partial fulfillment of the

requirements for the degree

MASTER OF SCIENCE

Department of Nuclear Engineering

KANSAS STATE UNIVERSITY
Manhattan, Kansas

1972

Approved by

Major Professor

TABLE OF CONTENTS

1.0 Introduction 1

2.0 Theory 2

3.0 Experimental Facilities and Equiptment 8

3.1 Fission Neutron Source 8

3.2 KSU NE-213 Fast-Neutron Spectrometer System 8

3.3 Experimental Configuration for Reflection Measurements 9

4.0 Data Collection and Analysis 14

4.1 Equipment Calibration 14

4.2 Experimental Procedures 15

4.3 Calculated Fast-Neutron Albedos 16

4.4 Orders-of-Scattering Calculations 16

5.0 Results and Discussion 18

5.1 Fast-Neutron Albedos for Steel and Concrete 18

5.2 Orders-of-Scattering Calculations 26

6.0 Suggestions for Further Study 53

7.0 Acknowledgements 54

8.0 References 55

9.0 Appendices 57

Appendix A: Cross Section Transformation Code, GETIT 58

Appendix B: Multi-Component Material Synthesis Code, MIXUP 62

Appendix C: Fast-Neutron Albedo Determination Code, ALBEE 64

1.0 INTRODUCTION

With the impending advent of the fast reactor a great need exists for reliable experimental fast-neutron penetration and reflection data. Theoretical calculations have been and are being performed in this area but until recently there had been no fast-neutron spectrometer systems available to obtain experimental reflection and penetration spectra for comparison with calculated spectra. Development of the NE-213 proton recoil liquid scintillation fast-neutron spectrometer has provided the means to obtain the needed experimental angular and energy dependent fast-neutron penetration and reflection data in the energy range 1 to 14 MeV in reasonable time and at reasonable expense.

In this work fast-neutron reflection spectra were measured for concrete and steel using the KSU NE-213 spectrometer system. From these data neutron dose albedos were calculated for thick slabs of steel and concrete. When theoretical calculations are performed to obtain reflected fast neutron spectra, the results need to be verified with a reliable set of experimental data. Thus the Monte Carlo calculated dose albedos were compared with the experimental albedos. In addition, calculations need to be performed to verify the experimental results. Therefore orders-of-scattering calculations were performed to generate fast-neutron reflection spectra for concrete and steel which were compared with experimental fast-neutron spectra.

2.0 THEORY

Two sets of comprehensive fast-neutron albedos established through Monte Carlo calculations exist. The accuracy of such Monte Carlo calculations, however, is only as good as the combined accuracy of the arithmetic code and the energy and angular dependent cross sections used.

The earliest detailed published Monte Carlo work was that of Allen et al[1] who calculated double differential number and dose albedos for four angles of incidence (θ_o = 0, 30, 45 and 70 degrees) and eight neutron source energies (E_o = 0.1, 0.25, 0.5, 1, 2, 3, 5 and 14 MeV). Allen's results are tabulated in terms of different energy sets, the energy spacing and range being dependent upon the source energy. For example, for a source energy of 1 MeV, the albedos are tabulated for the following energy bins: 0.00001-0.001, 0.001-0.025, 0.025-0.0625, 0.0625-0.1, 0.1-0.175, 0.175-0.25, 0.25-0.375, 0.375-0.5, 0.5-0.75, and 0.75-1.0 MeV. Five materials were studied: concrete, water, aluminum, iron, dry Nevada Test Site soil, 50% moisture saturated NTS soil, and 100% moisture saturated NTS soil.

Later Maerker et al[2] calculated double differential dose albedos for concrete using the 05R Oak Ridge Monte Carlo code. Five polar angles of incidence (θ_o = 0, 45, 60, 75, and 85 degrees), and six incident energy bins (ΔE_o = 0.2-0.75, 0.75-1.5, 1.5-3.0, 3.0-4.0, 4.0-6.0 and 6.0-8.0 MeV) were used in the Monte Carlo code. Albedos were reported for nine polar angles of reflection (161, 146, 136, 127, 120, 113, 106, 100, and 93 degrees), six azimuthal angles of reflection (15, 45, 105, 135 and 165 degrees) and ten reflected energy bins (0.2-0.4, 0.4-0.6, 0.6-0.8, 0.8-1.0, 1.0-1.5, 1.5-2, 2-3, 3-4, 4-6, and 6-8 MeV).

Experimental differential number albedos have been measured at the Oak Ridge Tower Shielding Facility using a fast-neutron dosimeter and a modified long counter. These results were converted to dose albedos using a Monte Carlo calculated reflected energy spectrum. At the time these measurements were made it was not possible to measure double differential number albedos directly because of the lack of an applicable neutron spectrometer.

A one dimensional S_n calculation of neutron spectra reflected from thick slabs was presented by Meyer et al.[3] These spectra calculations were completed for concrete and cold roll steel using the ANISN code. All of the ANISN calculations were made for quadrature order 16 (Gaussian-16 or Modified Lobatto-16) but P_0, P_4, P_6 and P_8 orders of anistropy were considered.

Bednarz and Kuszell[4] obtained a solution to the albedo problem with the boundary condition that is dependent on the angle of incidence and position on the irradiated plane. Kapen's technique of solution to the one-velocity, three dimensional isotropic scattering Boltzmann equation was used. The problem of periodic irradiation was considered as an example.

Song et al[5] presented a four-factor semiempirical formula derived by assuming the reflected neutrons could be represented by a linear combination of two terms; one term represented the singly scattered neutrons; the other term represented neutrons scattered many times before reflection. The differential neutron scattering cross section was approximated by a first order Legendre Polynomial in terms of the scattering angle. The results determined by this semiempirical formula were compared to the Monte Carlo results of Allen and were found to agree within 15% for all of the materials studied. The energy bins used by Allen and Song were found to be too complex for use in comparing their calculations with experimental results.

The orders-of-scattering technique developed by Thiesing[8] for fast-neutron transport assumes the neutrons scattered to the detector are linear combination of those neutrons that are singly scattered, those neutrons that are doubly scattered, etc. The order-of-scattering results (single and double scattering contributions) were found to agree within 5% with experimental results.

In this work experimental NE-213 results for concrete are compared to the ORNL 05R Monte Carlo calculated dose albedos of Maerker. The results of these Monte Carlo calculations are presented as double-differential dose albedos. To convert this data to a form that will permit comparison with the experimental results, a general equation was derived as follows:

$$D(E_j,\theta,\phi) = \frac{\sum_{n=1}^{5} \Delta E_n N(E_n) C(E_n) DD(E_n,E_j,\theta,\phi)}{\sum_{m=1}^{NGPS} \Delta E_m N(E_m) C(E_m)} \qquad (1)$$

where $N(E_n)$ = Number of neutron of energy E_n incident on the slab/cm^2 MeV

ΔE_n = Width of the n^{th} ORNL direct beam energy bin

$C(E_n)$ = Henderson's flux to dose conversion factor[6] corresponding to energy E_n

$DD(E_j,E_n,\theta,\phi)$ = ORNL Monte Carlo double-differential dose albedo

NGPS = Number of groups (48) in the FERDOR unfolding code between .8 and 8 MeV

The corresponding equation for calculating the dose albedo based on the KSU experimental data is

$$D(E_m,\theta,\phi) = \frac{\Phi(E_m) C(E_m) \frac{F_I}{F_{ref}}}{\frac{1}{R^2} \sum_{m=1}^{NGPS} \Delta E_m N(E_m) C(E_m)} \qquad (2)$$

where $\Phi(E_m)$ = Neutron flux reflected by the specimen slab intercepted by the detector in neutrons/cm^2 min.MeV (data obtained from FERDOR unfolded NE-213 measured results)

$\frac{F_I}{F_{ref}}$ = Normalization factor to account for power variances

R = Slab to detector distance (cm)

For ease of calculation and to conserve the structure of the spectra, the energy bin widths used in the presentation of experimental dose albedos were those utilized in the FERDOR[7] unfolding code (0.1 MeV from 1 to 3 MeV and 0.2 MeV above 3 MeV). For both Equations (1) and (2) the results are calculated in terms of dose per steradian per MeV per unit incident dose.

The orders-of-scattering technique developed by Thiesing[8] for neutron scattering was also used to provide a comparison with the experimental results. This technique assumes the neutrons scattered to the detector are linear combinations of those neutrons that are singly scattered, those neutrons that are doubly scattered, etc. The angular dependent scattering cross sections used in the orders-of-scattering calculations were expanded in a ninth order Legendre polynomial (P_8) and obtained from the Radiation Shielding Information Center multigroup cross section sets DLC-2B[9] and DLC-9[10].

The DLC-2B 99 group neutron cross section set[9] was used in the orders-of-scattering calculations for steel. Since the DLC-2B set did not include cross sections for two primary constituents of concrete, silicon and calcium, the DLC-9 122 group (104 neutron and 18 gamma ray) cross section set[10] was used in the orders-of-scattering calculations for concrete. The DLC-2B and DLC-9 cross section sets were generated from the ENDF/B evaluated

cross section library[11] using the SUPERTOG Code[12]. The SUPERTOG code generates grouped total and absorption cross sections using any weighting spectrum called for by the user. The cross section groups required to expand the energy range 1 to 15 MeV (27 groups of DLC-2B and 31 groups for DLC-9) were extracted from magnetic tape with the code GETIT. The code MIXUP was used to synthesize the steel and concrete from their respective elements using the appropriate number densities. Table 1 shows the group structure for the DLC-2B and DLC-9 cross section sets.

THIS BOOK
CONTAINS
NUMEROUS PAGES
WITH THE ORIGINAL
PRINTING BEING
SKEWED
DIFFERENTLY FROM
THE TOP OF THE
PAGE TO THE
BOTTOM.

THIS IS AS RECEIVED
FROM THE
CUSTOMER.

Table 1. Energy Structure used in the DLC-2B and DLC-9 grouped Cross Section Sets

Group Number	DLC-2B		DLC-9	
	Mean Energy (MeV)	Group Width (MeV)	Mean Energy (MeV)	Group Width (MeV)
1	14.208	1.421	14.249	1.501
2	12.856	1.286	12.856	1.285
3	11.633	1.163	11.633	1.162
4	10.526	1.053	10.526	1.052
5	9.524	0.952	9.524	0.952
6	8.618	0.862	8.618	0.861
7	7.798	0.780	7.798	0.779
8	7.056	0.706	7.204	0.408
9	6.384	0.638	6.852	0.307
10	5.777	0.578	6.532	0.350
11	5.227	0.523	6.213	0.317
12	4.730	0.473	5.777	0.287
13	4.280	0.428	5.227	0.259
14	3.872	0.387	4.858	0.116
15	3.504	0.350	4.622	0.119
16	3.170	0.317	4.279	0.212
17	2.869	0.287	3.072	0.297
18	2.596	0.260	3.504	0.343
19	2.349	0.235	3.171	0.295
20	2.125	0.212	2.869	0.577
21	1.923	0.192	2.595	0.522
22	1.740	0.174	2.408	0.216
23	1.574	0.157	2.291	0.257
24	1.424	0.142	2.125	0.427
25	1.289	0.129	1.923	0.192
26	1.166	0.117	1.740	0.174
27	1.055	0.105	1.574	0.157
28	0.955	0.095	1.424	0.142
29	0.864	0.086	1.289	0.129
30	0.782	0.078	1.160	0.116
31	0.707	0.071	1.055	0.105
32	0.640	0.064	0.955	0.095

3.0 EXPERIMENTAL FACILITIES AND EQUIPMENT

3.1 Fission Neutron Source

The northeast fast beam port ("C") of the 250 kW KSU TRIGA Mark II reactor was used as the source of fast neutrons. This radial beam port is aligned with a cylindrical void in the core reflector graphite and is nominally 8 inches in diameter at the reactor face. Since there is little material in the path of the neutrons coming from the core, the spectrum is essentially a fission spectrum with sufficient neutrons for experimental measurements up to an energy of 10 MeV. To reduce the gamma background while leaving the neutron spectrum essentially unaffected a 2 inch long bismuth plug was inserted in the end of the 1-1/4 inch square lead and borated paraffin collimator used during reflection measurements to collimate the incident beam.

3.2 KSU NE-213 Fast-Neutron Spectrometer System

Experimental measurements of fast-neutron reflection spectra were completed using the KSU NE-213 2 inch proton recoil, liquid scintillation fast-neutron spectrometer system. The system detector is a 2 by 2 inch cylindrical glass bottle filled with NE-213 proton recoil liquid scintillator coupled to an RCA 4810 14 dynode photomultiplier tube. A pulse shape discrimination circuit is used to distinguish between gamma ray and neutron pulses. The gamma ray interference is removed by requiring coincidence between pulses coming from the pulse shape discrimination circuit and the undistorted linear energy signal containing both gamma ray and neutron pulses.

The KSU detector and tube-base gamma ray discrimination circuit assembly are similar to those developed by Verbinski[13]. The operating principles of

the system, its energy resolution and its detection efficiency are discussed in various reports[13,14,15,16].

3.3 Experimental Configuration for Reflection Measurements

The slab mounting assembly developed by Simons[17] which allowed experiments to be carried out using any combination of angles θ_o, θ, and ϕ was utilized in all reflection measurements. For neutron reflection measurements for steel, a 24 x 24 x 6 inch slab of cold rolled steel was used. The concrete in the 26 x 26 x 9 inch slab used as a reflecting medium, was proportioned to rigid specifications, to approximate as closely as possible the compositions assumed in ORNL 05R Monte Carlo calculations of concrete albedos.[2] Measured KSU atomic densities (atoms/cm^3), water content, and specific gravity for the concrete were: Si, 10.14×10^{21}; O, 45.1×10^{21}; H, 10.41×10^{21}; C, 5.0×10^{2} water content, 6.4%; specific gravity, 2.4. During measurements the slab mount was positioned with the center point of the front face of the mounted slab seve feet (213.36 cm) from the reactor face on the beam port center line. To obtain the various experimental angles the specimen slab was tilted or rotated about the fixed front-face center point and the NE-213 detector moved in a quadrant to the right of the slab on a 5.5 foot (167.64 cm) radius (see Fig. 1). Table 2 shows the relationship between the experimental angles α, β, and γ and the corresponding polar coordinate angles θ_o, θ, and ϕ as shown in Fig. 2.

For each measurement of a reflected spectrum a room scattered background spectrum was also measured. This background measurement was accomplished by placing an iron and methyl methacrylate shielding cone between the detector and slab. The cone was fabricated from six two-inch thick iron plates decreasing in size from 12 x 12 inches to 7 x 7 inches plus six two-inch thick methyl methacrylate plates decreasing in size from 7 x 7 inches to

THIS BOOK CONTAINS NUMEROUS PICTURES THAT ARE ATTACHED TO DOCUMENTS CROOKED.

THIS IS AS RECEIVED FROM CUSTOMER.

Table 2. Experimental Angles α,β,γ and Corresponding Angles θ_o,θ,and ϕ.

θ_0(deg)	θ(deg)	ϕ(deg)	α(deg)	β(deg)	γ(deg)
0	106	---	0	16.1	73.9
0	120	---	0	30.0	60.0
0	127	---	0	37.7	52.3
0	146	---	0	56.4	33.6
0	160	---	0	70.8	19.2
45	136	135	42.1	76.1	31.2
45	160	15	3.8	71.4	63.5
60	113	105	57.1	46.1	66.3
60	127	135	51.8	87.6	37.8
75	120	105	59.5	79.6	69.8
75	146	105	33.4	92.6	69.3

THIS BOOK CONTAINS NUMEROUS PAGES WITH DIAGRAMS THAT ARE CROOKED COMPARED TO THE REST OF THE INFORMATION ON THE PAGE.

THIS IS AS RECEIVED FROM CUSTOMER.

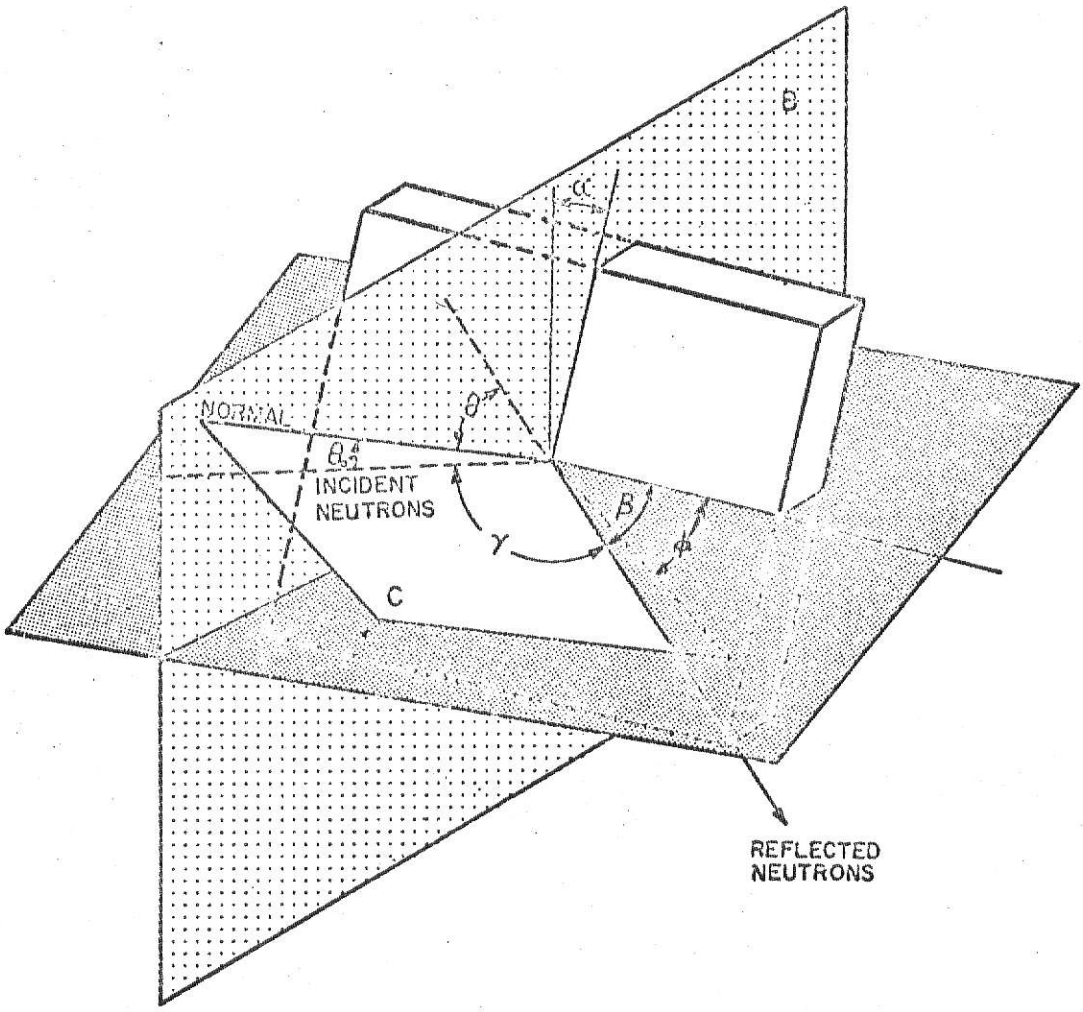

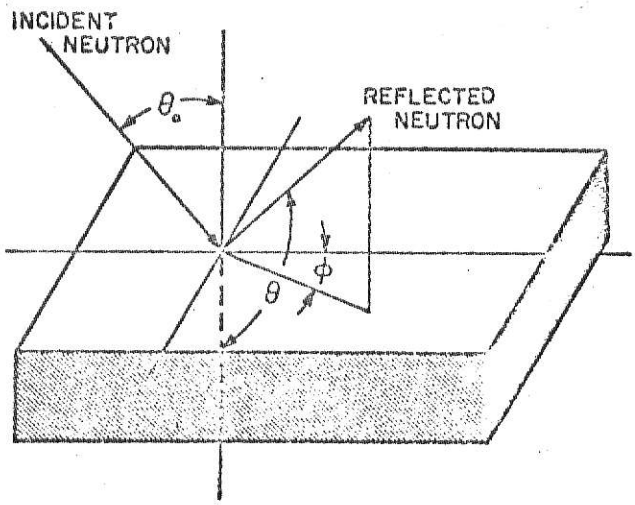

Figure 2. Geometry used in fast-neutron reflection studies and relationships between the experimental angles α, β and γ and θ_0, θ, ϕ.

2 x 2 inches. When in position the cone completely shielded or shadowed the 2 x 2 inch NE-213 detector from the slab. Simons[17] has shown that a negligible fraction of neutrons from the direct neutron beam leak through the shielding cone. Hence it was not necessary to correct background measurements for leakage through the cone. The position of the shielding cone during experimental background measurements is shown in Fig. 1.

4.0 DATA COLLECTION AND ANALYSIS

4.1 Equipment Calibration

A routine procedure has been established for obtaining a reliable NE-213 spectrometer system neutron spectrum during experimental measurements. This procedure establishes the spectrometer system energy calibration parameters, the necessary reactor power for the experiment and the integrated reactor flux.

Prior to calibration, the detection system was allowed to warm up for a twelve hour period. After this warm-up period a ^{60}Co gamma ray spectrum was measured and the extrapolated Compton tail was used to set the energy gain of the spectrometer system. The gamma ray rejection ratio was set at >150:1 using a ^{60}Co source; that is less than one ^{60}Co gamma ray in 150 in the linear energy circuit was counted. Before any experimental run a one hour PuBe spectrum was collected with the gamma ray rejection circuit operative. This test spectrum was compared to a standard complex PuBe spectrum (spectrum as measured and recorded in the multichannel pulse height analyzer) to insure that the system was working properly. A ^{60}Co spectrum was again taken before and after each experimental neutron spectrum to re-establish the gain and gamma ray rejection ratio.

Due to the radiation sensitivity of the Forte circuit and the photo-multiplier tube, the total radiation at the detector was kept below 3 mrem/hr. When the detection system was operating in the anticoincidence mode, a 10% dead time on the TMC 4096 multichannel pulse height analyzer (MCPHA) corresponded roughly to 3 mrem/hr at the detector. Thus the 10% dead time reading on the MCPHA was used to establish the maximum reactor power for all experimental runs.

The strip chart recorders used by the reactor operator to monitor the reactor power, measure only nominal reactor power and were thus not considered sufficiently accurate to give a direct measure of the integrated reactor power over the one hour period of an experimental run. Therefore nickel foils were used to monitor the fast neutron fluence in the reactor. The nickel reaction $^{58}Ni(n,p)^{58}Co$ has an effective neutron energy threshold of 2.9 MeV, and an effective cross section of 0.420 barn. Since it was desired to obtain a measure of the fast-neutron flux at the fast beam port of the reactor, this reaction with its high energy threshold was chosen to monitor the reactor fast-neutron level. ^{58}Co decays with a half-life of 71.4 days and gives off a 0.811 MeV gamma ray. Due to the relatively long half-life, this reaction could be used to monitor the fast-neutron level without considering ^{58}Co decay during irradiation and with no requirement to count the nickel foils immediately after irradiation.

For a detailed description of fast-neutron flux monitoring using nickel foils, the reader is referred to AEC document COO-2049-9.

4.2 Experimental Procedures

For each set of experimental angles a foreground and background spectrum and their corresponding ^{60}Co spectra were accumulated in 1024 channels of a TMC MCPHA. The data was read out on magnetic tape and subsequently converted to punched cards for ready use in further analyses. The computer code NUDASBIN[8] was then used to perform the following analysis steps:

1: Determine the extrapolated zero intercept of the ^{60}Co combined Compton tail measured by the NE-213 detector.

2: Shift the total pulse-height spectrum and the background spectrum to a standard gain.

3: Normalize the background measurement to the total spectrum measurement based on total neutron fluence using the nickel foil data.

4: Subtract the background spectrum from the total pulse-height spectrum.

5: Obtain the shifted net pulse-height spectrum on punched cards in a format compatible with the input requirements of the code used to unfold the complex pulse-height spectrum to obtain the differential neutron energy spectrum.

The FERDOR code[7], developed by Burrus at Oak Ridge National Laboratory, was used to unfold the complex pulse-height spectrum into the differential energy spectrum.

4.3 Calculated Fast-Neutron Albedos

A computer code, ALBEE, was written to calculate the experimental fast-neutron dose albedos based on Equation 2 and to permit comparison of the experimental measured albedos with the ORNL dose albedos calculated using Equation 1. All experimental fast-neutron spectra were normalized to a single direct neutron beam power level using the Ni foil data. Henderson's flux to dose conversion factors[6] were used in converting the measured number albedo results to dose albedos.

4.4 Orders-of-Scattering Calculations

Orders-of-scattering calculations were performed for steel and concrete. The single and double scattering contributions were assumed to represent the total number of neutrons scattered to the detector. The computer code SINGDET[8] was used to calculate the single scattered contribution to the flux at the detector. The code DOUBDET[8] was used to calculate the contribution made by the doubly scattered neutrons. The orders-of-scattering

calculated results were synthesized into reflected energy spectra using Thiesing's flux synthesis code[8]. The energy spectrum and total number of fast-neutrons incident on the specimen slabs were taken to be the same as those determined by Thiesing. The double scattered results were summed over the intermediate energy groups before being synthesized into reflected neutron spectra.

The total cross sections and 9 Legendre moments of the angular dependent scattering cross sections were taken from the DLC-2B 99 group cross section set for the steel calculations and from the DLC-9 122 group cross section set for the concrete orders-of-scattering calculations. The computer code GETIT was used to extract the first 34 cross section groups from each cross section set. The steel and concrete cross sections were synthesized from their respective component cross sections with the code MIXUP. The number densities ($\times 10^{-24}$) used for steel of density 7.7 gm/cm^3 were N_{Fe} = 0.081793 atoms/cm^3 and N_C = 0.00579183 atoms/cm^3. For concrete the constituent number densities were N_{Si} = 0.001014 atoms/cm^3, N_{Ca} = 0.00753 atoms/cm^3, N_H = 0.01041 atoms/cm^3, N_O = 0.0451 atoms/cm^3, and N_C = 0.0050 atoms/cm^3.

5.0 RESULTS AND DISCUSSION

5.1 Fast-Neutron Albedos for Steel and Concrete

Steel and concrete fast-neutron dose albedos were calculated from experimental spectra according to Equation 2. Experimental steel fast-neutron albedos did not exhibit any particular structure over the energy range of interest, 0.8 to 8 MeV (see Fig. 3-4). Although the iron cross-section data exhibit many close packed resonance peaks in the MeV region, the NE-213 detector data as unfolded by the FERDOR code are not capable of resolving the fine structure of the scattered neutron spectra resulting from the iron resonances and thus the observed smooth spectra would be expected. KSU experimental reflected dose albedos for steel are summarized in Tables 3-4.

All of the measured concrete reflected dose albedos exhibit a broad peak at about 2.5 MeV (see Fig. 5). This peak is primarily a result of fast-neutrons back-scattering from oxygen, the major constituent in the concrete. The oxygen cross section has a wide resonance peak between 3 and 4 MeV which would scatter 3 to 4 MeV neutrons into about the 3.1 to 2.3 MeV energy region. In addition, the oxygen cross section contains a deep minimum at about 2.3 MeV which would allow fast-neutron scattered into the 2.3 MeV energy region to penetrate long distances into the concrete with little chance of being back scattered again. Also carbon scattered fast-neutrons would contribute to the 2.0 to 2.2 MeV region structure by resonance scattering of 2.7 to 3.2 MeV neutrons. Calcium and silicon would tend to uniformly back scatter fast-neutrons. The final concrete constituent, hydrogen, whose albedo is zero, indirectly influences the number of back-scattered neutrons by decreasing the total number of back-scattered neutrons.

Figure 3. Fast-Neutron Energy and Angular Dependent Dose Albedos from 15.24 cm Thick Steel Slab

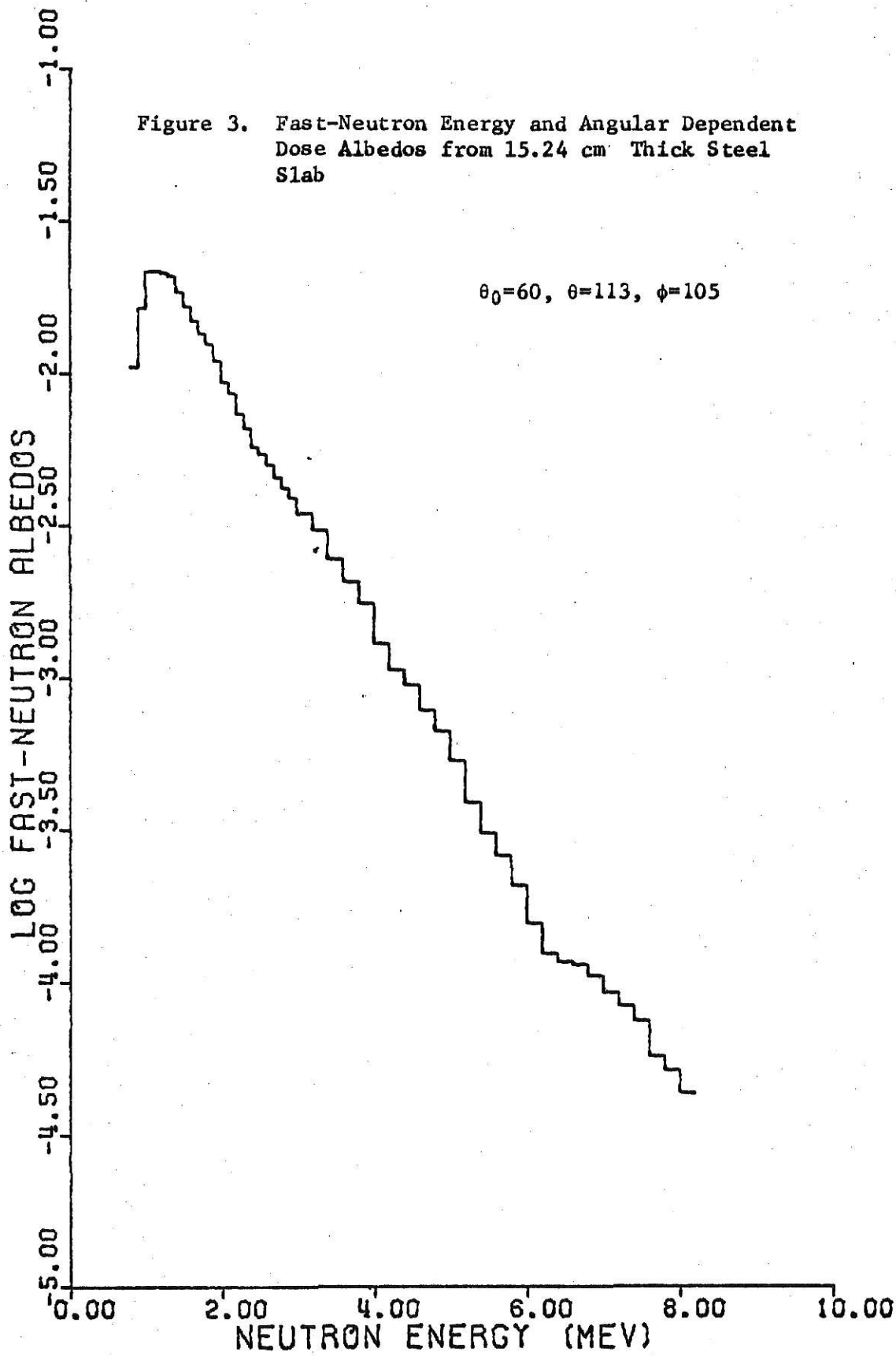

Figure 4. Fast-Neutron Energy and Angular Dependent Dose Albedos from 15.24 cm Thick Steel Slab

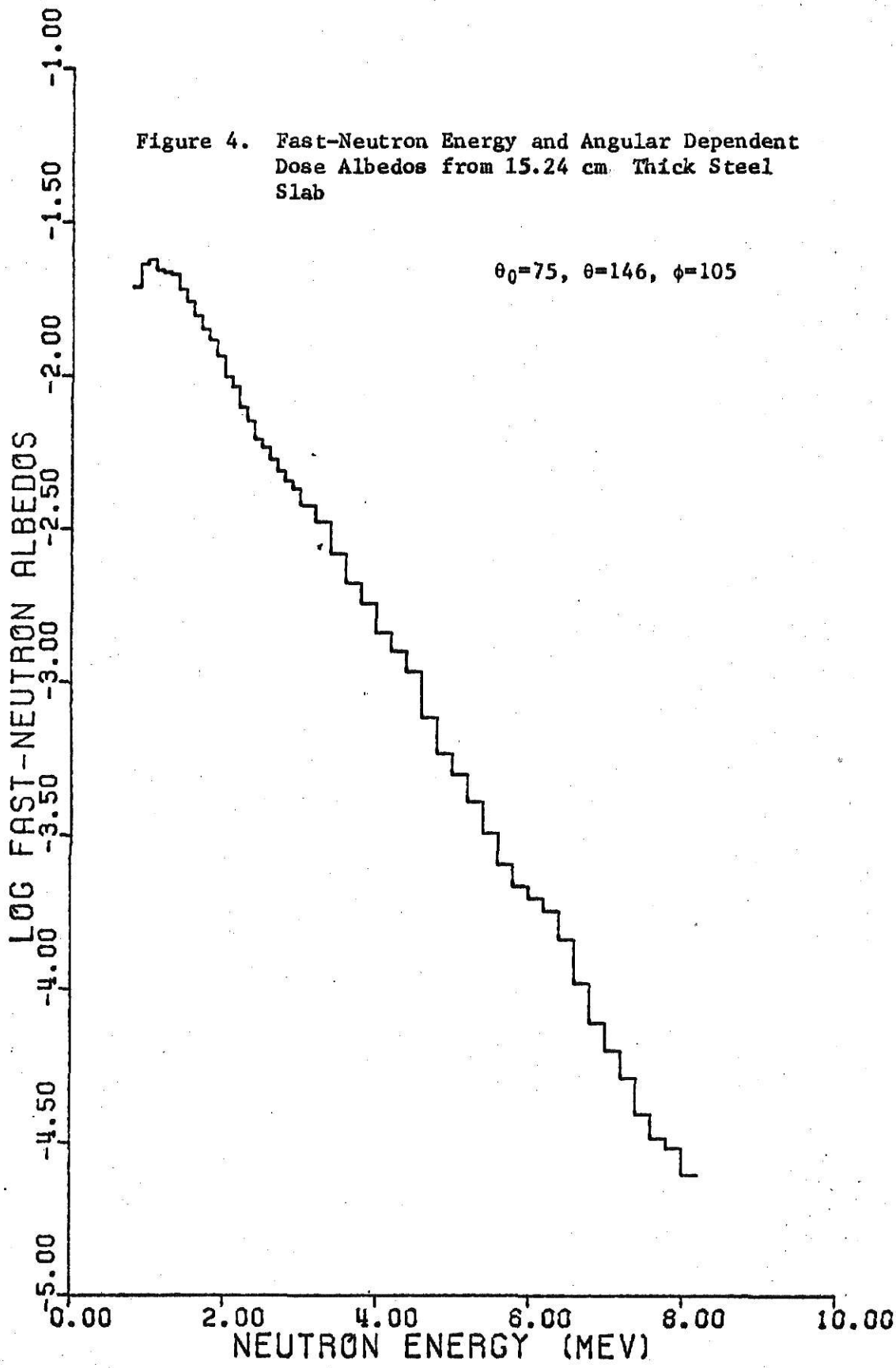

Table 3. Experimental Fast-Neutron Angular and Energy Dependent Dose Albedos for Steel (reflected dose/str MeV/unit incident dose)

	θ_i=0.0 θ^o=160.8	θ_i=0.0 θ^o=106.1	θ_i=0.0 θ^o=127.7	θ_i=0.0 θ^o=146.4	θ_i=0.0 θ^o=120.0
1	0.577×10^{-2}	0.805×10^{-2}	0.672×10^{-2}	0.102×10^{-1}	0.586×10^{-2}
2	0.607×10^{-2}	0.915×10^{-2}	0.904×10^{-2}	0.123×10^{-1}	0.886×10^{-2}
3	0.582×10^{-2}	0.899×10^{-2}	0.982×10^{-2}	0.124×10^{-1}	0.105×10^{-2}
4	0.515×10^{-2}	0.895×10^{-2}	0.872×10^{-2}	0.108×10^{-1}	0.962×10^{-2}
5	0.490×10^{-2}	0.772×10^{-2}	0.829×10^{-2}	0.107×10^{-1}	0.963×10^{-2}
6	0.469×10^{-2}	0.762×10^{-2}	0.806×10^{-2}	0.108×10^{-1}	0.995×10^{-2}
7	0.404×10^{-2}	0.675×10^{-2}	0.712×10^{-2}	0.968×10^{-2}	0.907×10^{-2}
8	0.352×10^{-2}	0.599×10^{-2}	0.637×10^{-2}	0.869×10^{-2}	0.817×10^{-2}
9	0.307×10^{-2}	0.527×10^{-2}	0.563×10^{-2}	0.768×10^{-2}	0.711×10^{-2}
10	0.267×10^{-2}	0.462×10^{-2}	0.499×10^{-2}	0.688×10^{-2}	0.623×10^{-2}
11	0.240×10^{-2}	0.412×10^{-2}	0.453×10^{-2}	0.628×10^{-2}	0.560×10^{-2}
12	0.213×10^{-2}	0.359×10^{-2}	0.401×10^{-2}	0.548×10^{-2}	0.491×10^{-2}
13	0.184×10^{-2}	0.309×10^{-2}	0.345×10^{-2}	0.460×10^{-2}	0.421×10^{-2}
14	0.168×10^{-2}	0.289×10^{-2}	0.317×10^{-2}	0.413×10^{-2}	0.413×10^{-2}
15	0.142×10^{-2}	0.250×10^{-2}	0.266×10^{-2}	0.347×10^{-2}	0.323×10^{-2}
16	0.125×10^{-2}	0.227×10^{-2}	0.231×10^{-2}	0.307×10^{-2}	0.285×10^{-2}
17	0.108×10^{-2}	0.195×10^{-2}	0.196×10^{-2}	0.265×10^{-2}	0.245×10^{-2}
18	0.101×10^{-2}	0.181×10^{-2}	0.182×10^{-2}	0.248×10^{-2}	0.227×10^{-2}
19	0.926×10^{-3}	0.161×10^{-2}	0.169×10^{-2}	0.222×10^{-2}	0.183×10^{-2}
20	0.859×10^{-3}	0.142×10^{-2}	0.158×10^{-2}	0.194×10^{-2}	0.183×10^{-2}
21	0.813×10^{-3}	0.128×10^{-2}	0.149×10^{-2}	0.169×10^{-2}	0.168×10^{-2}
22	0.764×10^{-3}	0.118×10^{-2}	0.138×10^{-2}	0.146×10^{-2}	0.151×10^{-2}
23	0.674×10^{-3}	0.106×10^{-2}	0.120×10^{-2}	0.122×10^{-2}	0.126×10^{-2}
24	0.585×10^{-3}	0.953×10^{-3}	0.102×10^{-2}	0.106×10^{-2}	0.944×10^{-3}
25	0.471×10^{-3}	0.776×10^{-3}	0.800×10^{-3}	0.877×10^{-3}	0.742×10^{-3}
26	0.388×10^{-3}	0.645×10^{-3}	0.629×10^{-3}	0.728×10^{-3}	0.629×10^{-3}
27	0.332×10^{-3}	0.541×10^{-3}	0.480×10^{-3}	0.599×10^{-3}	0.489×10^{-3}
28	0.258×10^{-3}	0.400×10^{-3}	0.344×10^{-3}	0.424×10^{-3}	0.354×10^{-3}
29	0.213×10^{-3}	0.320×10^{-3}	0.300×10^{-3}	0.330×10^{-3}	0.318×10^{-3}
30	0.167×10^{-3}	0.250×10^{-3}	0.274×10^{-3}	0.285×10^{-3}	0.245×10^{-3}

Table 3. (continued)

31	0.118×10^{-3}	0.190×10^{-3}	0.215×10^{-3}	0.241×10^{-3}	0.151×10^{-3}
32	0.105×10^{-3}	0.175×10^{-3}	0.168×10^{-3}	0.208×10^{-3}	0.148×10^{-3}
33	0.988×10^{-4}	0.158×10^{-3}	0.125×10^{-3}	0.141×10^{-3}	0.141×10^{-3}
34	0.779×10^{-4}	0.115×10^{-3}	0.948×10^{-4}	0.125×10^{-3}	0.103×10^{-3}
35	0.593×10^{-4}	0.764×10^{-4}	0.834×10^{-4}	0.990×10^{-4}	0.905×10^{-4}
36	0.452×10^{-4}	0.569×10^{-4}	0.719×10^{-4}	0.820×10^{-4}	0.880×10^{-4}
37	0.322×10^{-4}	0.491×10^{-4}	0.534×10^{-4}	0.681×10^{-4}	0.818×10^{-4}
38	0.223×10^{-4}	0.432×10^{-4}	0.354×10^{-4}	0.573×10^{-4}	0.798×10^{-4}
39	0.181×10^{-4}	0.375×10^{-4}	0.272×10^{-4}	0.538×10^{-4}	0.752×10^{-4}
40	0.181×10^{-4}	0.340×10^{-4}	0.274×10^{-4}	0.547×10^{-4}	0.639×10^{-4}
41	0.189×10^{-4}	0.333×10^{-4}	0.276×10^{-4}	0.514×10^{-4}	0.551×10^{-4}
42	0.197×10^{-4}	0.327×10^{-4}	0.244×10^{-4}	0.435×10^{-4}	0.436×10^{-4}
43	0.193×10^{-4}	0.277×10^{-4}	0.192×10^{-4}	0.351×10^{-4}	0.354×10^{-4}
44	0.169×10^{-4}	0.232×10^{-4}	0.156×10^{-4}	0.275×10^{-4}	0.314×10^{-4}
45	0.127×10^{-4}	0.195×10^{-4}	0.139×10^{-4}	0.212×10^{-4}	0.293×10^{-4}
46	0.977×10^{-5}	0.158×10^{-4}	0.117×10^{-4}	0.175×10^{-4}	0.271×10^{-4}
47	0.697×10^{-5}	0.120×10^{-4}	0.898×10^{-4}	0.144×10^{-4}	0.239×10^{-4}
48	0.697×10^{-5}	0.960×10^{-5}	0.789×10^{-4}	0.112×10^{-4}	0.196×10^{-4}

Table 4. Experimental Fast-Neutron Angular and Energy Dependent Dose Albedos for Steel (reflected dose/str. MeV/unit incident dose)

	θ =45 θ^{o}=160 ϕ =15	θ =45 θ^{o}=136 ϕ =135	θ =60 θ^{o}=127 ϕ =135	θ =60 θ^{o}=113 ϕ =105	θ =75 θ^{o}=120 ϕ =105	θ =75 θ^{o}=146 ϕ =105
1	0.494×10^{-2}	0.667×10^{-2}	0.547×10^{-2}	0.350×10^{-2}	0.420×10^{-2}	0.195×10^{-2}
2	0.541×10^{-2}	0.875×10^{-2}	0.844×10^{-2}	0.546×10^{-2}	0.655×10^{-2}	0.232×10^{-2}
3	0.534×10^{-2}	0.932×10^{-2}	0.101×10^{-1}	0.720×10^{-2}	0.864×10^{-2}	0.240×10^{-2}
4	0.476×10^{-2}	0.850×10^{-2}	0.970×10^{-2}	0.718×10^{-2}	0.858×10^{-2}	0.221×10^{-2}
5	0.456×10^{-2}	0.848×10^{-2}	0.977×10^{-2}	0.710×10^{-2}	0.861×10^{-2}	0.218×10^{-1}
6	0.445×10^{-2}	0.848×10^{-2}	0.972×10^{-2}	0.695×10^{-2}	0.860×10^{-2}	0.214×10^{-1}
7	0.392×10^{-2}	0.752×10^{-2}	0.862×10^{-2}	0.614×10^{-2}	0.767×10^{-2}	0.192×10^{-1}
8	0.352×10^{-2}	0.671×10^{-2}	0.774×10^{-2}	0.550×10^{-2}	0.692×10^{-2}	0.175×10^{-1}
9	0.309×10^{-2}	0.599×10^{-2}	0.697×10^{-2}	0.493×10^{-2}	0.626×10^{-2}	0.157×10^{-1}
10	0.273×10^{-2}	0.544×10^{-2}	0.633×10^{-2}	0.448×10^{-2}	0.571×10^{-2}	0.142×10^{-1}
11	0.248×10^{-2}	0.506×10^{-2}	0.584×10^{-2}	0.414×10^{-2}	0.528×10^{-2}	0.131×10^{-1}
12	0.218×10^{-2}	0.447×10^{-2}	0.518×10^{-2}	0.365×10^{-2}	0.467×10^{-2}	0.115×10^{-1}
13	0.189×10^{-2}	0.374×10^{-2}	0.447×10^{-2}	0.311×10^{-2}	0.400×10^{-2}	0.995×10^{-2}
14	0.176×10^{-2}	0.341×10^{-2}	0.408×10^{-2}	0.286×10^{-2}	0.375×10^{-2}	0.923×10^{-2}
15	0.151×10^{-2}	0.292×10^{-2}	0.342×10^{-2}	0.245×10^{-2}	0.325×10^{-2}	0.792×10^{-2}
16	0.132×10^{-2}	0.266×10^{-2}	0.298×10^{-2}	0.219×10^{-2}	0.298×10^{-2}	0.715×10^{-2}
17	0.113×10^{-2}	0.230×10^{-2}	0.253×10^{-2}	0.191×10^{-2}	0.262×10^{-2}	0.623×10^{-2}
18	0.107×10^{-2}	0.209×10^{-2}	0.232×10^{-2}	0.180×10^{-2}	0.246×10^{-2}	0.586×10^{-2}
19	0.990×10^{-3}	0.183×10^{-2}	0.209×10^{-2}	0.166×10^{-2}	0.223×10^{-2}	0.535×10^{-2}
20	0.913×10^{-3}	0.157×10^{-2}	0.187×10^{-2}	0.152×10^{-2}	0.200×10^{-2}	0.489×10^{-2}
21	0.847×10^{-3}	0.138×10^{-2}	0.172×10^{-2}	0.140×10^{-2}	0.182×10^{-2}	0.453×10^{-2}
22	0.777×10^{-3}	0.122×10^{-2}	0.156×10^{-2}	0.129×10^{-2}	0.165×10^{-2}	0.426×10^{-2}
23	0.677×10^{-3}	0.104×10^{-2}	0.133×10^{-2}	0.115×10^{-2}	0.145×10^{-2}	0.377×10^{-2}
24	0.576×10^{-3}	0.862×10^{-3}	0.105×10^{-2}	0.101×10^{-2}	0.128×10^{-2}	0.335×10^{-2}
25	0.457×10^{-3}	0.686×10^{-3}	0.818×10^{-3}	0.813×10^{-3}	0.104×10^{-2}	0.263×10^{-2}
26	0.387×10^{-3}	0.599×10^{-3}	0.683×10^{-3}	0.686×10^{-3}	0.891×10^{-3}	0.210×10^{-2}
27	0.330×10^{-3}	0.530×10^{-3}	0.563×10^{-3}	0.583×10^{-3}	0.813×10^{-3}	0.181×10^{-2}
28	0.236×10^{-3}	0.377×10^{-3}	0.409×10^{-3}	0.429×10^{-3}	0.630×10^{-3}	0.145×10^{-2}
29	0.192×10^{-3}	0.277×10^{-3}	0.344×10^{-3}	0.352×10^{-3}	0.517×10^{-3}	0.126×10^{-2}
30	0.168×10^{-3}	0.225×10^{-3}	0.315×10^{-3}	0.314×10^{-3}	0.537×10^{-3}	0.109×10^{-2}

Table 4 (continued)

31	0.126×10^{-3}	0.177×10^{-3}	0.241×10^{-3}	0.259×10^{-3}	0.315×10^{-3}	0.764×10^{-3}
32	0.988×10^{-4}	0.148×10^{-3}	0.177×10^{-3}	0.221×10^{-3}	0.239×10^{-3}	0.584×10^{-3}
33	0.795×10^{-4}	0.133×10^{-3}	0.137×10^{-3}	0.177×10^{-3}	0.185×10^{-3}	0.498×10^{-3}
34	0.614×10^{-4}	0.733×10^{-4}	0.108×10^{-3}	0.128×10^{-3}	0.142×10^{-3}	0.406×10^{-3}
35	0.497×10^{-4}	0.544×10^{-4}	0.800×10^{-4}	0.102×10^{-3}	0.120×10^{-3}	0.322×10^{-3}
36	0.416×10^{-4}	0.572×10^{-4}	0.513×10^{-4}	0.861×10^{-4}	0.103×10^{-3}	0.254×10^{-3}
37	0.343×10^{-4}	0.689×10^{-4}	0.343×10^{-4}	0.689×10^{-4}	0.915×10^{-4}	0.215×10^{-3}
38	0.275×10^{-4}	0.715×10^{-4}	0.331×10^{-4}	0.518×10^{-4}	0.857×10^{-4}	0.198×10^{-3}
39	0.237×10^{-4}	0.594×10^{-4}	0.357×10^{-4}	0.411×10^{-4}	0.772×10^{-4}	0.180×10^{-4}
40	0.227×10^{-4}	0.409×10^{-4}	0.336×10^{-4}	0.386×10^{-4}	0.730×10^{-4}	0.145×10^{-3}
41	0.211×10^{-4}	0.300×10^{-4}	0.312×10^{-4}	0.378×10^{-4}	0.629×10^{-4}	0.105×10^{-3}
42	0.175×10^{-4}	0.281×10^{-4}	0.282×10^{-4}	0.347×10^{-4}	0.478×10^{-4}	0.775×10^{-4}
43	0.140×10^{-4}	0.249×10^{-4}	0.244×10^{-4}	0.306×10^{-4}	0.365×10^{-4}	0.631×10^{-4}
44	0.110×10^{-4}	0.217×10^{-4}	0.215×10^{-4}	0.277×10^{-4}	0.293×10^{-4}	0.515×10^{-4}
45	0.867×10^{-5}	0.185×10^{-4}	0.197×10^{-4}	0.248×10^{-4}	0.261×10^{-4}	0.392×10^{-4}
46	0.712×10^{-5}	0.153×10^{-4}	0.165×10^{-4}	0.190×10^{-4}	0.255×10^{-4}	0.327×10^{-4}
47	0.534×10^{-5}	0.138×10^{-4}	0.121×10^{-4}	0.170×10^{-4}	0.226×10^{-4}	0.304×10^{-4}
48	0.430×10^{-5}	0.118×10^{-4}	0.942×10^{-5}	0.144×10^{-4}	0.200×10^{-4}	0.248×10^{-4}

Figure 5. Fast-Neutron Energy and Angular Dependent Dose Albedos from 22.86 cm Thick Concrete Slab

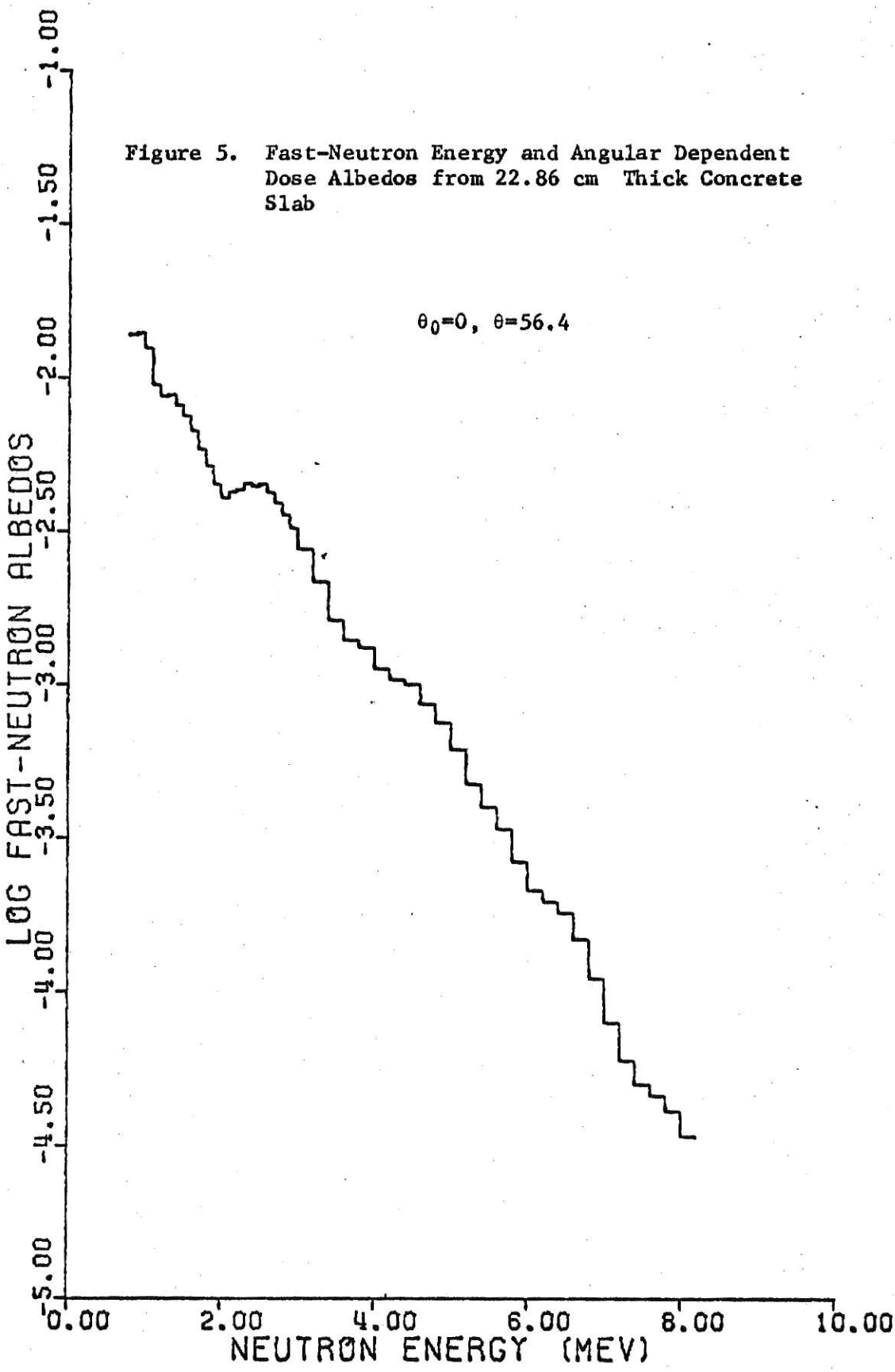

The KSU measured dose albedos for concrete were compared to the 05R Monte Carlo dose albedos calculated by Maerker at ORNL. The results of this comparison are shown in Fig. 6-11. The measured concrete dose albedos are tabulated in Tables 5-6. In all cases the KSU measured dose albedos lie below (on the average a factor of 70-80% lower) the corresponding ORNL Monte Carlo calculated dose albedos. One possible reason for this difference would be the large energy bin widths used in the Monte Carlo results. Also the Monte Carlo results were based on point cross sections and not on the multi-group cross section sets which have been updated and are presently considered to be more accurate. In particular the oxygen cross sections used in the Monte Carlo calculations have been shown to be in error by as much as 65%[18]. The depth of the oxygen minimum was under predicted by a factor of about 70%[15]. Thus a significant error in terms of the number of neutrons forward scattering in oxygen interactions would be present in the Monte Carlo results.

5.2 Orders-of-Scattering Calculations

The single and double scattering results of Thiesing[8] were used to verify the normalization of the experimental spectra for the reflection of fast-neutrons from steel. The orders-of-scattering calculations for steel were carried out using the DLC-2B 99 group neutron cross sections. Figures 12-13 show the comparison between the orders-of-scattering calculations and the experimental measurements both in energy spectrum and absolute magnitude. Very good agreement in both spectral shape and absolute magnitude was found between the orders-of-scattering calculations and the experimental measurements. The differences in magnitude at 6.5 to 8 MeV are known to be caused by numerical noise in the unfolding procedure used to analyze the complex pulse height spectra.

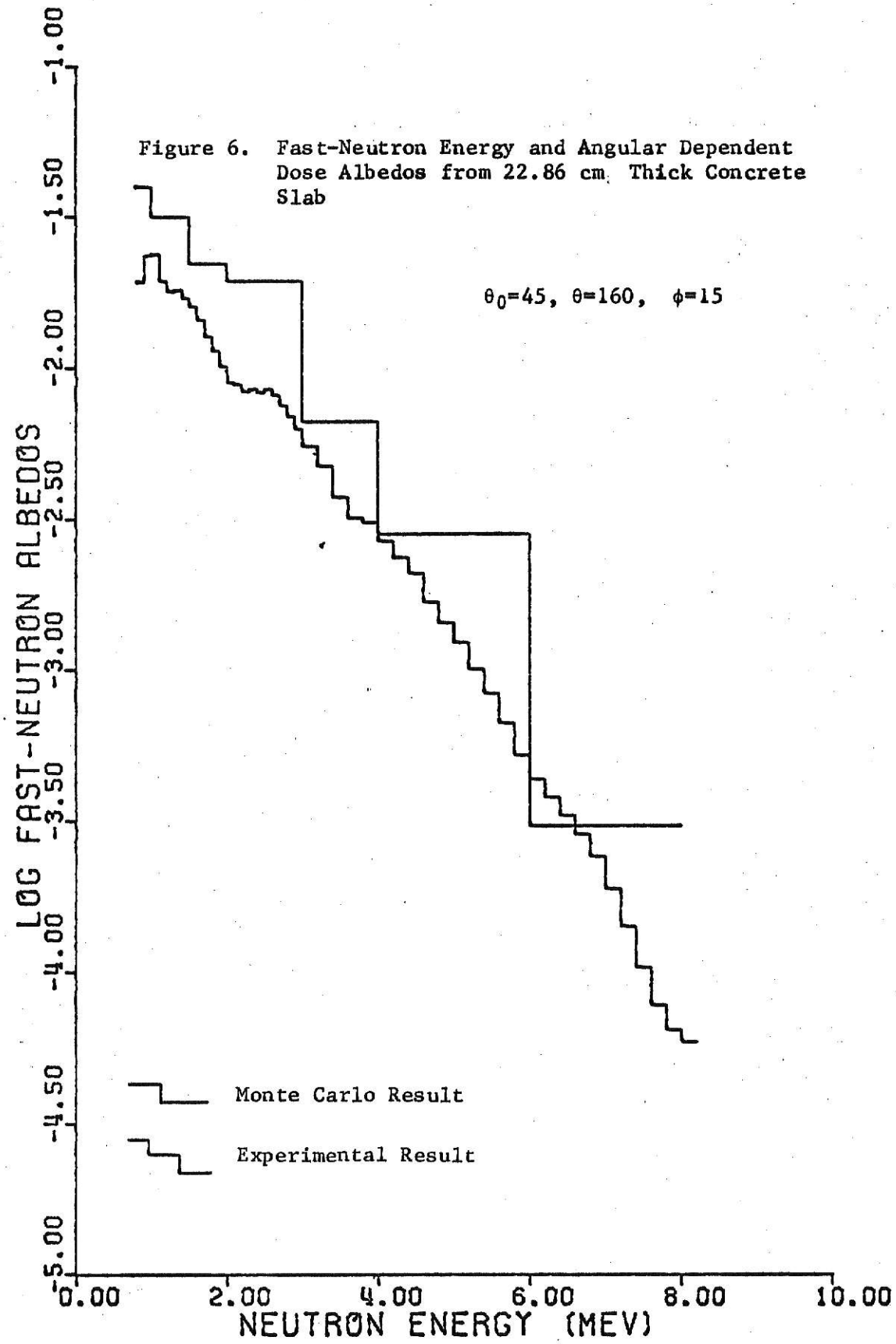

Figure 6. Fast-Neutron Energy and Angular Dependent Dose Albedos from 22.86 cm Thick Concrete Slab

Figure 7. Fast-Neutron Energy and Angular Dependent Dose Albedos from 22.86 cm Thick Concrete Slab

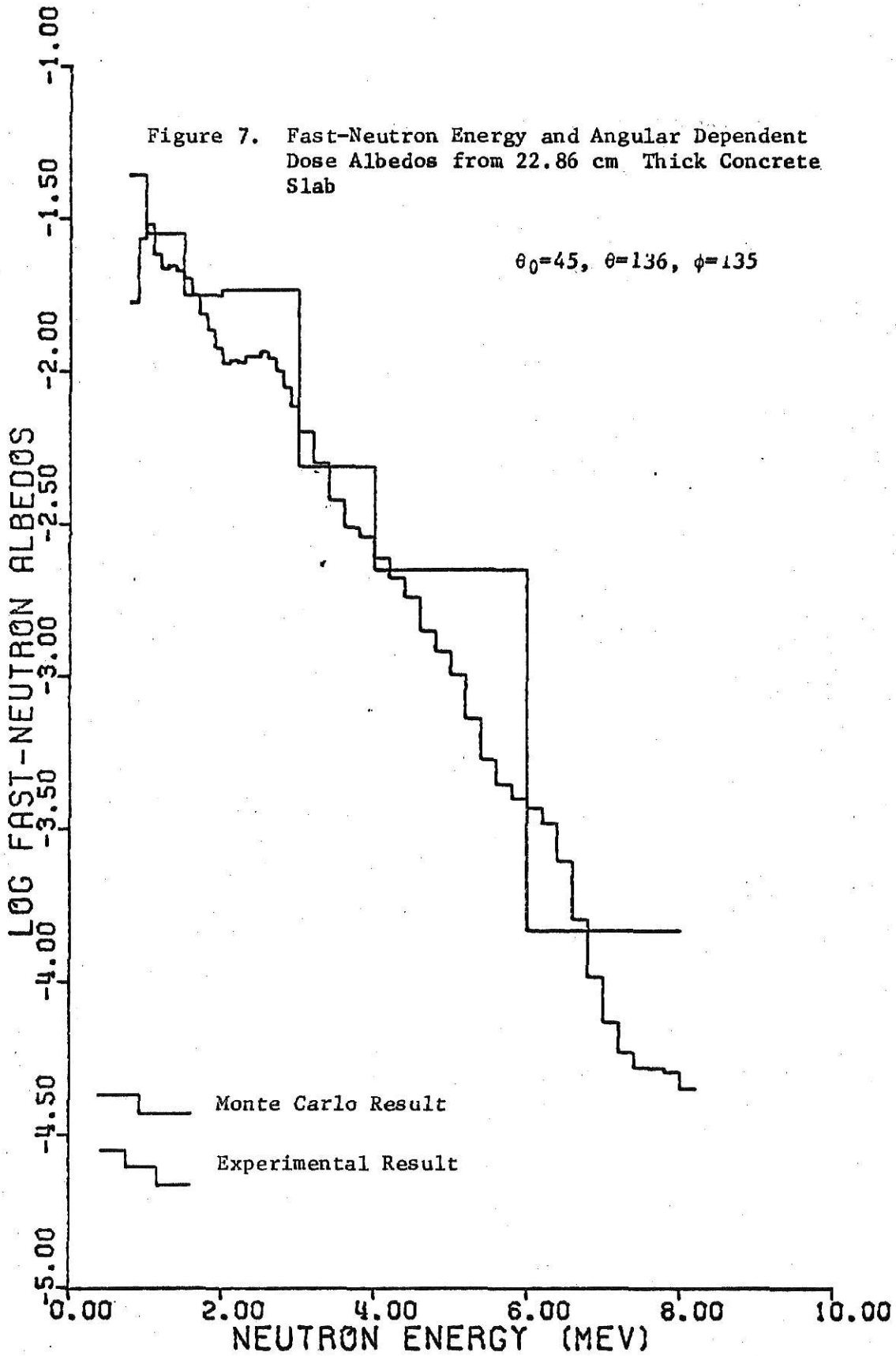

Figure 8. Fast-Neutron Energy and Angular Dependent Dose Albedos from 22.86 cm Thick Concrete Slab

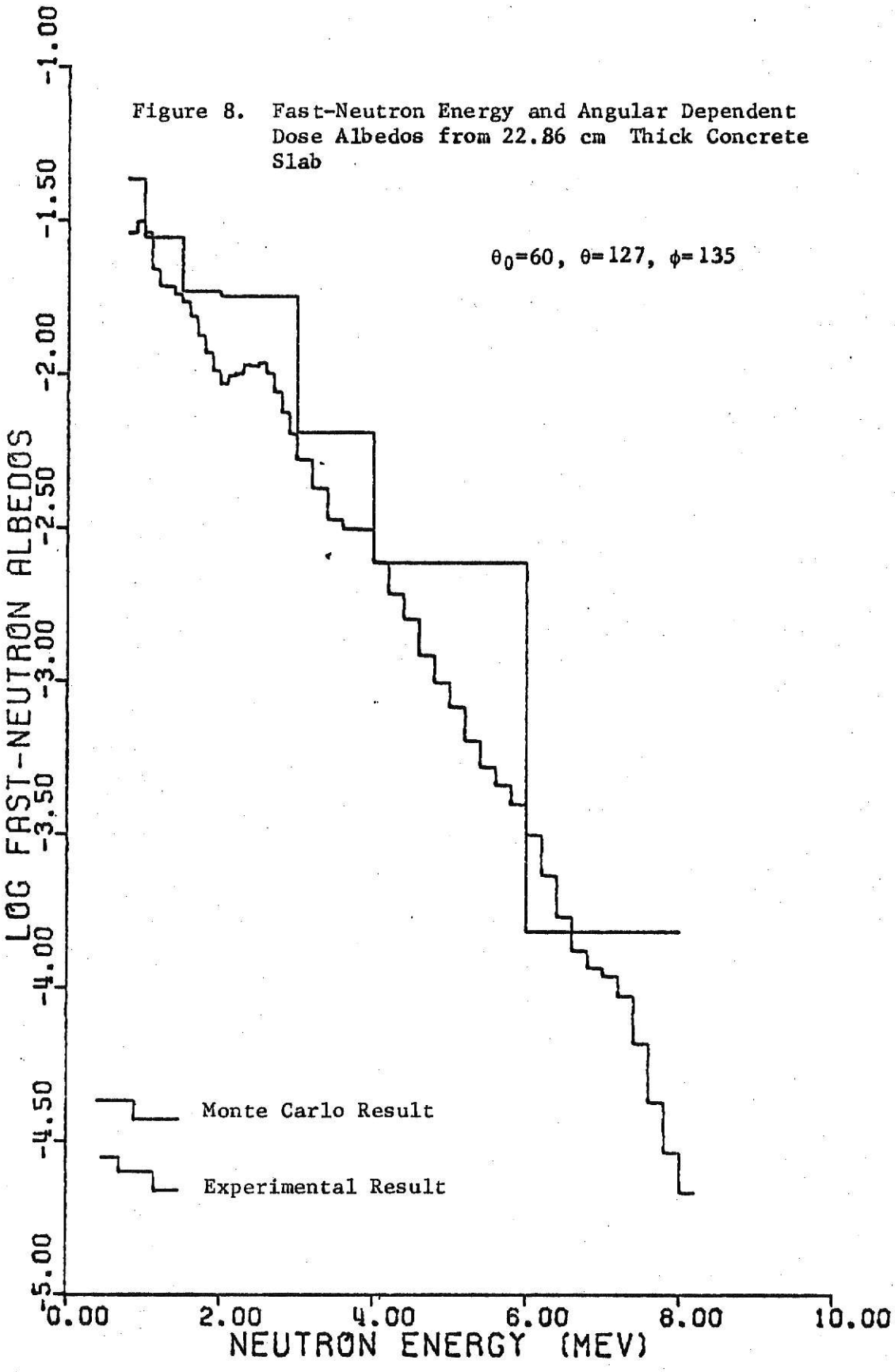

Figure 9. Fast-Neutron Energy And Angular Dependent Dose Albedos from 22.86 cm Thick Concrete Slab

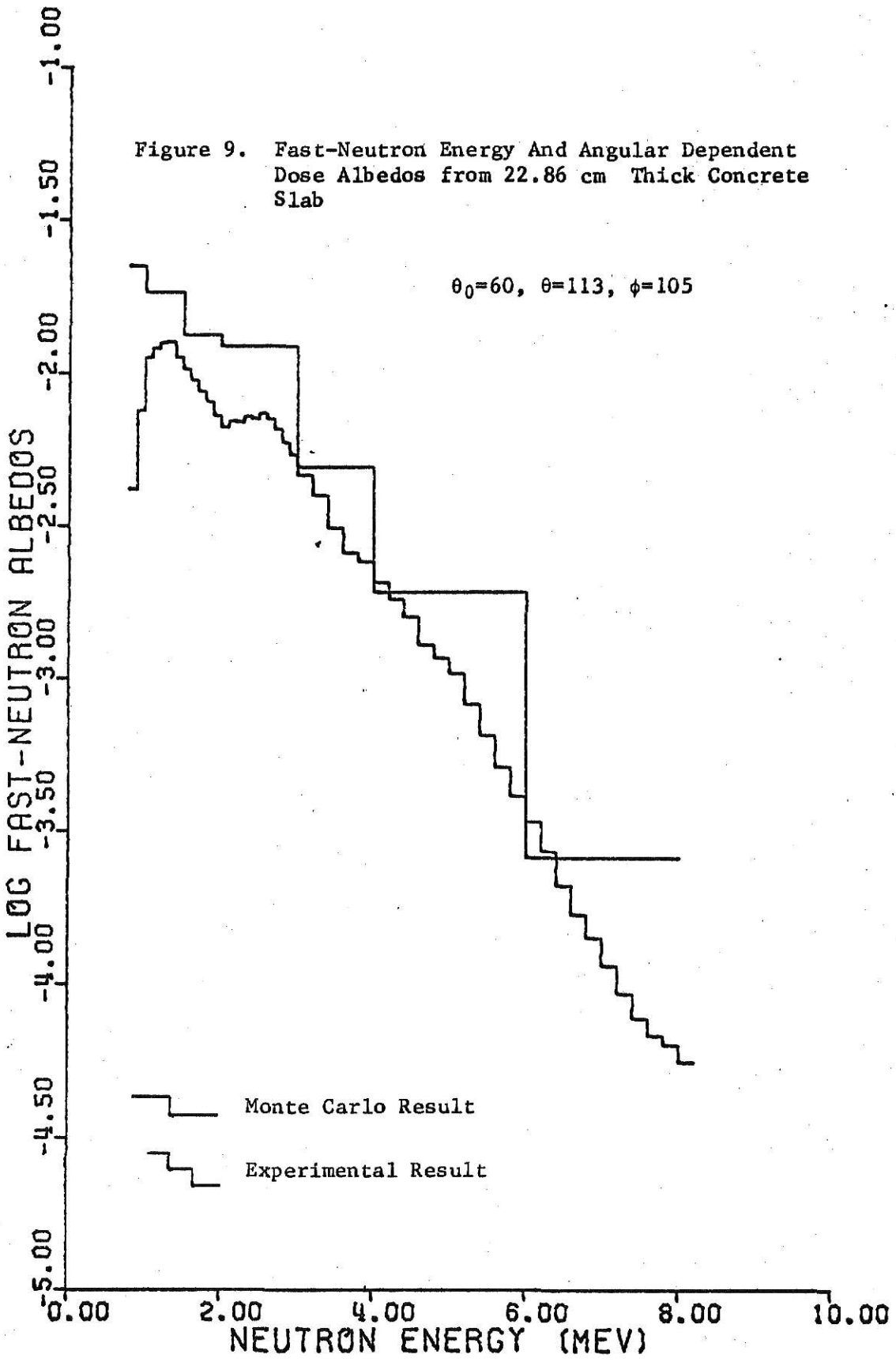

Figure 10. Fast-Neutron Energy and Angular Dependent Dose Albedos from 22.86 cm Thick Concrete Slab

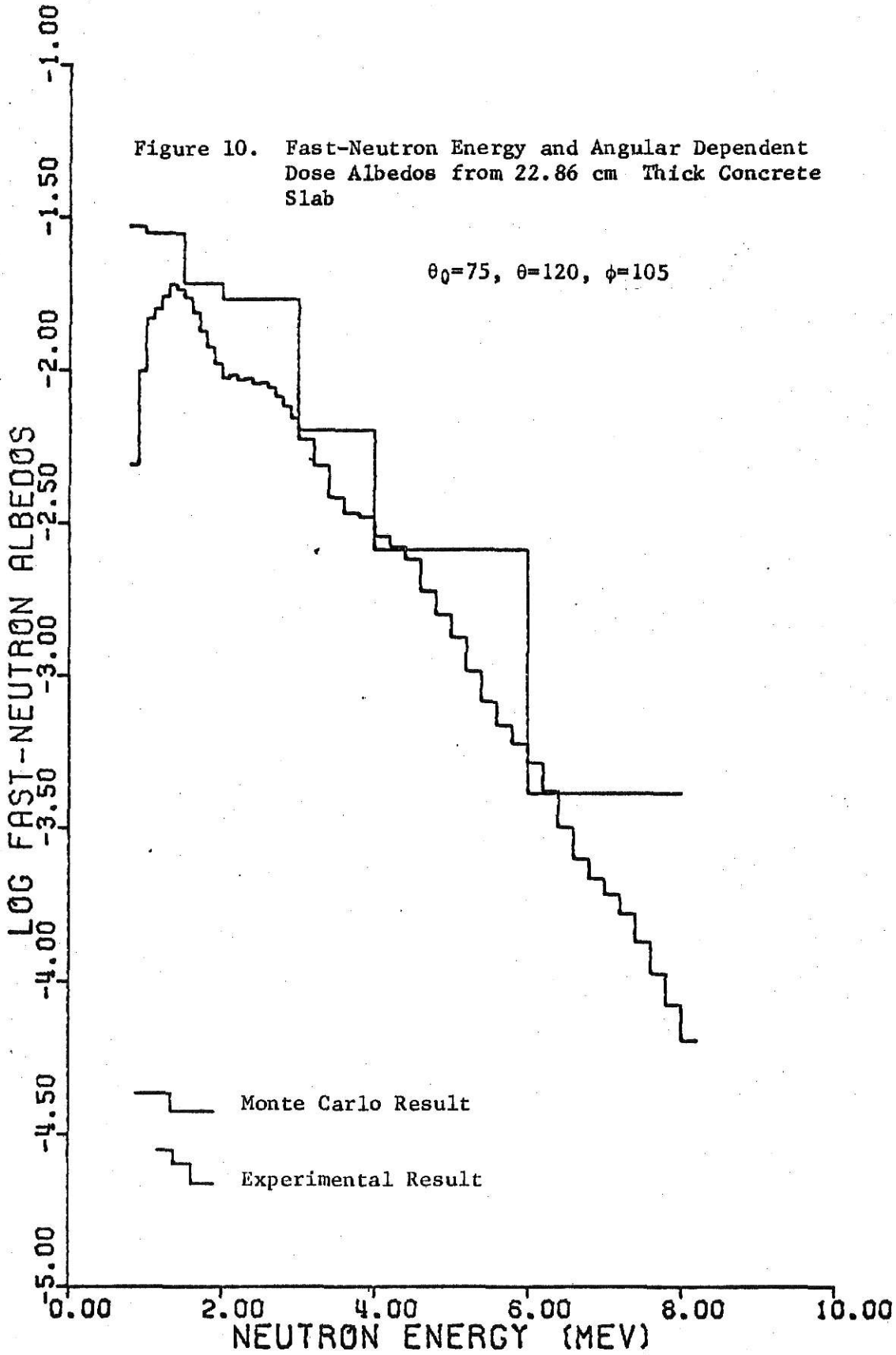

Figure 11. Fast-Neutron Energy and Angular Dependent Dose Albedos from 22.86 cm. Thick Concrete Slab

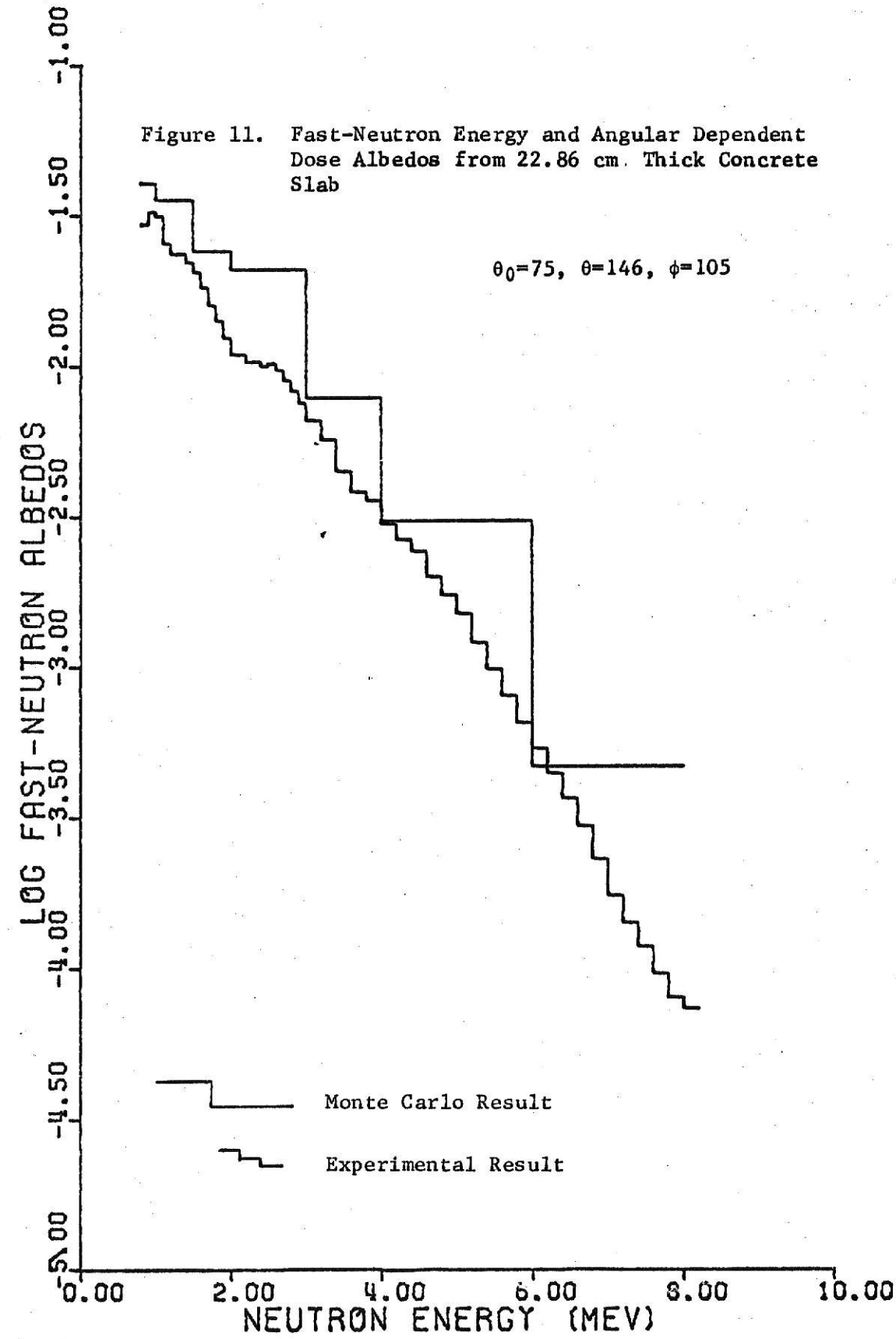

Table 5. Experimental Fast-Neutron Angular and Energy Dependent Dose Albedos for Concrete (reflected dose/str MeV/unit incident dose)

	θ_o=0.0 θ^o=160.8	θ_o=0.0 θ^o=106.1	θ_o=0.0 θ^o=127.7	θ_o=0.0 θ^o=146.4	θ_o=0.0 θ^o=120.0
1	0.297×10^{-2}	0.460×10^{-2}	0.291×10^{-2}	0.103×10^{-1}	0.697×10^{-2}
2	0.542×10^{-2}	0.467×10^{-2}	0.474×10^{-2}	0.113×10^{-1}	0.750×10^{-2}
3	0.645×10^{-2}	0.416×10^{-2}	0.625×10^{-2}	0.105×10^{-1}	0.105×10^{-2}
4	0.499×10^{-2}	0.317×10^{-2}	0.615×10^{-2}	0.777×10^{-2}	0.528×10^{-2}
5	0.440×10^{-2}	0.291×10^{-2}	0.572×10^{-2}	0.669×10^{-2}	0.474×10^{-2}
6	0.445×10^{-2}	0.294×10^{-2}	0.520×10^{-2}	0.653×10^{-2}	0.477×10^{-2}
7	0.423×10^{-2}	0.271×10^{-2}	0.455×10^{-2}	0.609×10^{-2}	0.450×10^{-2}
8	0.395×10^{-2}	0.250×10^{-2}	0.398×10^{-2}	0.571×10^{-2}	0.422×10^{-2}
9	0.343×10^{-2}	0.224×10^{-2}	0.361×10^{-2}	0.513×10^{-2}	0.375×10^{-2}
10	0.293×10^{-2}	0.195×10^{-2}	0.311×10^{-2}	0.444×10^{-2}	0.325×10^{-2}
11	0.261×10^{-2}	0.171×10^{-2}	0.277×10^{-2}	0.389×10^{-2}	0.289×10^{-2}
12	0.226×10^{-2}	0.150×10^{-2}	0.248×10^{-2}	0.337×10^{-2}	0.258×10^{-2}
13	0.198×10^{-2}	0.135×10^{-2}	0.224×10^{-2}	0.305×10^{-2}	0.235×10^{-2}
14	0.205×10^{-2}	0.142×10^{-2}	0.230×10^{-2}	0.323×10^{-2}	0.241×10^{-2}
15	0.212×10^{-2}	0.144×10^{-2}	0.224×10^{-2}	0.326×10^{-2}	0.234×10^{-2}
16	0.235×10^{-2}	0.151×10^{-2}	0.231×10^{-2}	0.344×10^{-2}	0.241×10^{-2}
17	0.245×10^{-2}	0.148×10^{-2}	0.227×10^{-2}	0.342×10^{-2}	0.235×10^{-2}
18	0.260×10^{-2}	0.150×10^{-2}	0.232×10^{-2}	0.348×10^{-2}	0.241×10^{-2}
19	0.252×10^{-2}	0.141×10^{-2}	0.221×10^{-2}	0.327×10^{-2}	0.230×10^{-2}
20	0.232×10^{-2}	0.130×10^{-2}	0.201×10^{-2}	0.295×10^{-2}	0.210×10^{-2}
21	0.206×10^{-2}	0.119×10^{-2}	0.182×10^{-2}	0.258×10^{-2}	0.189×10^{-2}
22	0.173×10^{-2}	0.108×10^{-2}	0.164×10^{-2}	0.225×10^{-2}	0.168×10^{-2}
23	0.133×10^{-2}	0.920×10^{-3}	0.141×10^{-2}	0.185×10^{-2}	0.143×10^{-2}
24	0.916×10^{-3}	0.719×10^{-3}	0.118×10^{-2}	0.144×10^{-2}	0.117×10^{-2}
25	0.753×10^{-3}	0.540×10^{-3}	0.880×10^{-3}	0.110×10^{-2}	0.895×10^{-3}
26	0.632×10^{-3}	0.464×10^{-3}	0.711×10^{-3}	0.935×10^{-3}	0.737×10^{-3}
27	0.496×10^{-3}	0.438×10^{-3}	0.656×10^{-3}	0.875×10^{-3}	0.666×10^{-3}
28	0.440×10^{-3}	0.374×10^{-3}	0.550×10^{-3}	0.689×10^{-3}	0.559×10^{-3}
29	0.400×10^{-3}	0.344×10^{-3}	0.499×10^{-3}	0.559×10^{-3}	0.503×10^{-3}
30	0.372×10^{-3}	0.332×10^{-3}	0.467×10^{-3}	0.471×10^{-3}	0.452×10^{-3}

Table 5 (continued)

31	0.317×10^{-3}	0.287×10^{-3}	0.371×10^{-3}	0.356×10^{-3}	0.360×10^{-3}
32	0.293×10^{-3}	0.248×10^{-3}	0.290×10^{-3}	0.296×10^{-3}	0.315×10^{-3}
33	0.259×10^{-3}	0.203×10^{-3}	0.228×10^{-3}	0.257×10^{-3}	0.276×10^{-3}
34	0.203×10^{-3}	0.157×10^{-3}	0.176×10^{-3}	0.201×10^{-3}	0.217×10^{-3}
35	0.169×10^{-3}	0.132×10^{-3}	0.142×10^{-3}	0.158×10^{-3}	0.170×10^{-3}
36	0.147×10^{-3}	0.112×10^{-3}	0.117×10^{-3}	0.127×10^{-3}	0.135×10^{-3}
37	0.113×10^{-3}	0.876×10^{-4}	0.960×10^{-4}	0.107×10^{-3}	0.110×10^{-3}
38	0.960×10^{-4}	0.709×10^{-4}	0.852×10^{-4}	0.996×10^{-4}	0.938×10^{-4}
39	0.767×10^{-4}	0.649×10^{-4}	0.795×10^{-4}	0.938×10^{-4}	0.784×10^{-4}
40	0.656×10^{-4}	0.597×10^{-4}	0.705×10^{-4}	0.775×10^{-4}	0.637×10^{-4}
41	0.521×10^{-4}	0.490×10^{-4}	0.562×10^{-4}	0.538×10^{-4}	0.551×10^{-4}
42	0.435×10^{-4}	0.367×10^{-4}	0.398×10^{-4}	0.340×10^{-4}	0.496×10^{-4}
43	0.352×10^{-4}	0.263×10^{-4}	0.348×10^{-4}	0.214×10^{-4}	0.402×10^{-4}
44	0.272×10^{-4}	0.199×10^{-4}	0.309×10^{-4}	0.158×10^{-4}	0.283×10^{-4}
45	0.257×10^{-4}	0.166×10^{-4}	0.283×10^{-4}	0.142×10^{-4}	0.179×10^{-4}
46	0.234×10^{-4}	0.152×10^{-4}	0.262×10^{-4}	0.139×10^{-4}	0.122×10^{-4}
47	0.212×10^{-4}	0.136×10^{-4}	0.216×10^{-4}	0.132×10^{-4}	0.108×10^{-4}
48	0.172×10^{-4}	0.113×10^{-4}	0.158×10^{-4}	0.116×10^{-4}	0.104×10^{-4}

Table 6. Experimental Fast-Neutron Angular and Energy Dependent Dose Albedos for Concrete (reflected dose/str MeV/unit incident dose)

	θ_i =45 θ^o=160 ϕ =15	θ_i =45 θ^o=136 ϕ =135	θ_i =60 θ^o=127 ϕ =135	θ_i =60 θ^o=113 ϕ =105	θ_i =75 θ^o=120 ϕ =105	θ_i =75 θ^o=146 ϕ =105
1	0.645×10^{-2}	0.565×10^{-2}	0.962×10^{-2}	0.139×10^{-2}	0.164×10^{-2}	0.109×10^{-2}
2	0.789×10^{-2}	0.913×10^{-2}	0.105×10^{-1}	0.252×10^{-2}	0.332×10^{-2}	0.109×10^{-1}
3	0.794×10^{-2}	0.102×10^{-1}	0.965×10^{-2}	0.378×10^{-2}	0.492×10^{-2}	0.105×10^{-1}
4	0.648×10^{-2}	0.809×10^{-2}	0.730×10^{-2}	0.403×10^{-2}	0.528×10^{-2}	0.849×10^{-2}
5	0.598×10^{-2}	0.728×10^{-2}	0.644×10^{-2}	0.421×10^{-2}	0.580×10^{-2}	0.783×10^{-2}
6	0.605×10^{-2}	0.742×10^{-2}	0.642×10^{-2}	0.423×10^{-2}	0.634×10^{-2}	0.788×10^{-2}
7	0.570×10^{-2}	0.714×10^{-2}	0.607×10^{-2}	0.376×10^{-2}	0.611×10^{-2}	0.736×10^{-2}
8	0.533×10^{-2}	0.674×10^{-2}	0.572×10^{-2}	0.344×10^{-2}	0.575×10^{-2}	0.683×10^{-2}
9	0.481×10^{-2}	0.596×10^{-2}	0.513×10^{-2}	0.316×10^{-2}	0.514×10^{-2}	0.608×10^{-2}
10	0.424×10^{-2}	0.513×10^{-2}	0.445×10^{-2}	0.290×10^{-2}	0.446×10^{-2}	0.579×10^{-2}
11	0.381×10^{-2}	0.455×10^{-2}	0.391×10^{-2}	0.269×10^{-2}	0.395×10^{-2}	0.471×10^{-2}
12	0.338×10^{-2}	0.398×10^{-2}	0.341×10^{-2}	0.242×10^{-2}	0.349×10^{-2}	0.414×10^{-2}
13	0.299×10^{-2}	0.355×10^{-2}	0.309×10^{-2}	0.222×10^{-2}	0.313×10^{-2}	0.365×10^{-2}
14	0.295×10^{-2}	0.363×10^{-2}	0.329×10^{-2}	0.232×10^{-2}	0.321×10^{-2}	0.364×10^{-2}
15	0.279×10^{-2}	0.359×10^{-2}	0.335×10^{-2}	0.231×10^{-2}	0.309×10^{-2}	0.344×10^{-2}
16	0.284×10^{-2}	0.375×10^{-2}	0.357×10^{-2}	0.240×10^{-2}	0.312×10^{-2}	0.345×10^{-2}
17	0.277×10^{-2}	0.375×10^{-2}	0.354×10^{-2}	0.237×10^{-2}	0.300×10^{-2}	0.333×10^{-2}
18	0.284×10^{-2}	0.388×10^{-2}	0.362×10^{-2}	0.246×10^{-2}	0.303×10^{-2}	0.340×10^{-2}
19	0.271×10^{-2}	0.369×10^{-2}	0.334×10^{-2}	0.236×10^{-2}	0.291×10^{-2}	0.323×10^{-2}
20	0.250×10^{-2}	0.335×10^{-2}	0.291×10^{-2}	0.218×10^{-2}	0.273×10^{-2}	0.299×10^{-2}
21	0.230×10^{-2}	0.296×10^{-2}	0.249×10^{-2}	0.198×10^{-2}	0.253×10^{-2}	0.275×10^{-2}
22	0.209×10^{-2}	0.257×10^{-2}	0.212×10^{-2}	0.180×10^{-2}	0.231×10^{-2}	0.251×10^{-2}
23	0.183×10^{-2}	0.212×10^{-2}	0.175×10^{-2}	0.155×10^{-2}	0.198×10^{-2}	0.220×10^{-2}
24	0.158×10^{-2}	0.167×10^{-2}	0.142×10^{-2}	0.133×10^{-2}	0.162×10^{-2}	0.189×10^{-2}
25	0.124×10^{-2}	0.126×10^{-2}	0.112×10^{-2}	0.104×10^{-2}	0.128×10^{-2}	0.149×10^{-2}
26	0.106×10^{-2}	0.106×10^{-2}	0.105×10^{-2}	0.860×10^{-3}	0.113×10^{-2}	0.127×10^{-2}
27	0.103×10^{-2}	0.962×10^{-3}	0.104×10^{-2}	0.803×10^{-3}	0.110×10^{-2}	0.119×10^{-2}
28	0.889×10^{-3}	0.816×10^{-3}	0.810×10^{-3}	0.687×10^{-3}	0.951×10^{-3}	0.995×10^{-3}
29	0.784×10^{-3}	0.703×10^{-3}	0.639×10^{-3}	0.605×10^{-3}	0.876×10^{-3}	0.881×10^{-3}
30	0.694×10^{-3}	0.606×10^{-3}	0.528×10^{-3}	0.530×10^{-3}	0.797×10^{-3}	0.806×10^{-3}

Table 6 (continued)

31	0.557×10^{-3}	0.470×10^{-3}	0.402×10^{-3}	0.428×10^{-3}	0.627×10^{-3}	0.666×10^{-3}
32	0.477×10^{-3}	0.402×10^{-3}	0.328×10^{-3}	0.388×10^{-3}	0.524×10^{-3}	0.578×10^{-3}
33	0.410×10^{-3}	0.337×10^{-3}	0.272×10^{-3}	0.345×10^{-3}	0.441×10^{-3}	0.500×10^{-3}
34	0.334×10^{-3}	0.242×10^{-3}	0.211×10^{-3}	0.273×10^{-3}	0.432×10^{-3}	0.401×10^{-3}
35	0.277×10^{-3}	0.177×10^{-3}	0.174×10^{-3}	0.215×10^{-3}	0.272×10^{-3}	0.327×10^{-3}
36	0.222×10^{-3}	0.148×10^{-3}	0.152×10^{-3}	0.170×10^{-3}	0.227×10^{-3}	0.266×10^{-3}
37	0.173×10^{-3}	0.133×10^{-3}	0.132×10^{-3}	0.136×10^{-3}	0.198×10^{-3}	0.217×10^{-3}
38	0.144×10^{-3}	0.124×10^{-3}	0.104×10^{-3}	0.113×10^{-3}	0.172×10^{-3}	0.178×10^{-3}
39	0.126×10^{-3}	0.110×10^{-3}	0.770×10^{-4}	0.903×10^{-4}	0.139×10^{-3}	0.147×10^{-3}
40	0.109×10^{-3}	0.824×10^{-4}	0.565×10^{-4}	0.699×10^{-4}	0.106×10^{-3}	0.122×10^{-3}
41	0.949×10^{-4}	0.532×10^{-4}	0.438×10^{-4}	0.562×10^{-4}	0.830×10^{-4}	0.987×10^{-4}
42	0.802×10^{-4}	0.346×10^{-4}	0.387×10^{-4}	0.470×10^{-4}	0.716×10^{-4}	0.766×10^{-4}
43	0.629×10^{-4}	0.247×10^{-4}	0.364×10^{-4}	0.381×10^{-4}	0.637×10^{-4}	0.580×10^{-4}
44	0.471×10^{-4}	0.197×10^{-4}	0.313×10^{-4}	0.309×10^{-4}	0.550×10^{-4}	0.470×10^{-4}
45	0.345×10^{-4}	0.175×10^{-4}	0.220×10^{-4}	0.257×10^{-4}	0.444×10^{-4}	0.393×10^{-4}
46	0.258×10^{-4}	0.174×10^{-4}	0.141×10^{-4}	0.226×10^{-4}	0.351×10^{-4}	0.319×10^{-4}
47	0.215×10^{-4}	0.170×10^{-4}	0.968×10^{-5}	0.211×10^{-4}	0.278×10^{-4}	0.266×10^{-4}
48	0.196×10^{-4}	0.150×10^{-4}	0.714×10^{-5}	0.185×10^{-4}	0.213×10^{-4}	0.245×10^{-4}

Figure 12. Fast-Neutron Reflection from 15.24 cm Thick Steel Slab

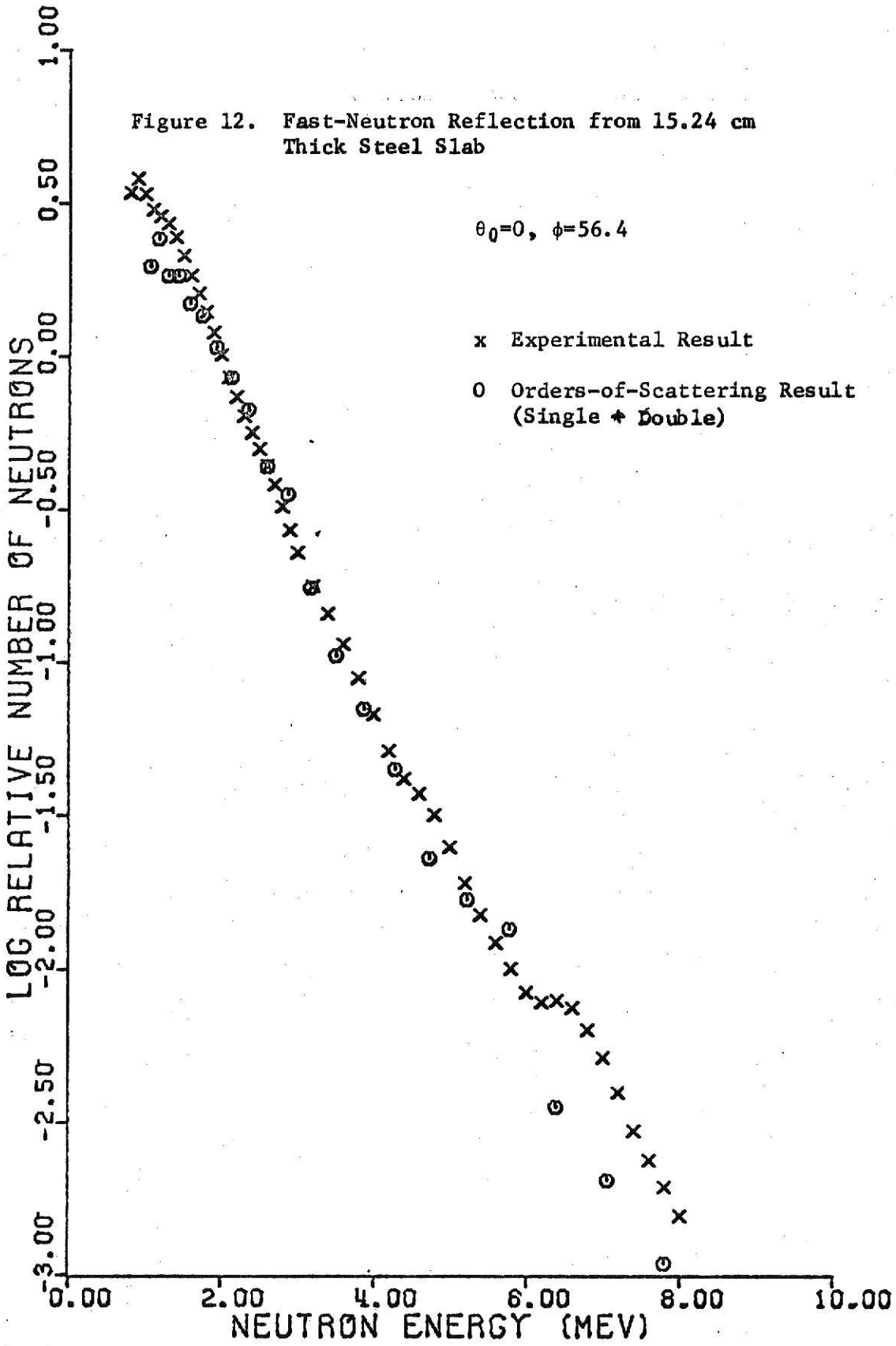

Figure 13. Fast-Neutron Reflection from 15.24 cm. Thick Steel Slab

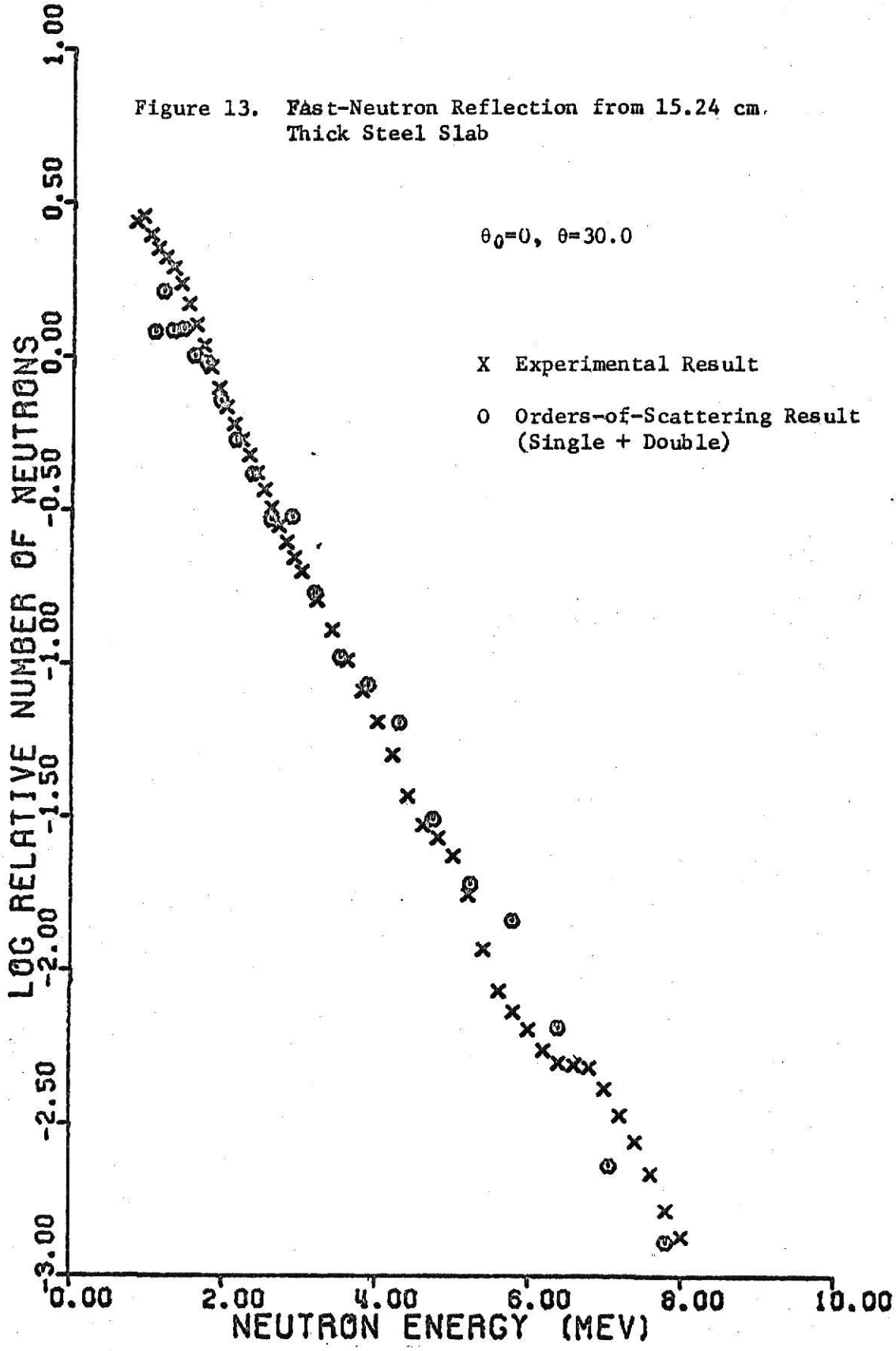

An attempt was made to perform the orders-of-scattering calculations for concrete to verify the concrete measurement normalization. Since the DLC-2B multigroup cross section set used by Thiesing did not include two primary constituents of concrete, calcium and silicon, the DLC-9 122 group (104 neutron and 18 gamma ray energy groups) cross section set was requested and received from the ORNL Radiation Shielding Information Center. The total cross sections and 9 Legendre moments (P_8) of the angular dependent scattering cross section for each constituent material of concrete from DLC-9 were multiplied by their measured respective number density (atoms/cm^3) to synthesize cross sections for concrete of the same composition as that used in the experimental measurements.

In addition to reflection calculations single and double-scatter calculations were made for a 45 degree penetration through concrete. These results were synthesized using the direct neutron beam spectra determined by Thiesing to be incident on the specimen slab; this is shown in Fig. 14. The extreme spectral structure noted in Fig. 14 around 2 MeV and the broad "peak" at 4 to 5 MeV could not be explained based on the known cross section structure of the concrete constituents thus an extensive analysis of the cross section retrieval codes and the single scattering code was undertaken to determine the probably cause of the observed structure. In addition a 30 degree reflection problem was completed using the single scattering code, SINGDET, to determine the general shape of the resulting synthesized spectrum. The calculated 30 degree reflection spectrum shown in Fig. 15 reveals an even stranger and unexplainable shape.

Careful study of the data on the original tape from which the DLC-9 cross sections were taken showed that the cross section extraction code

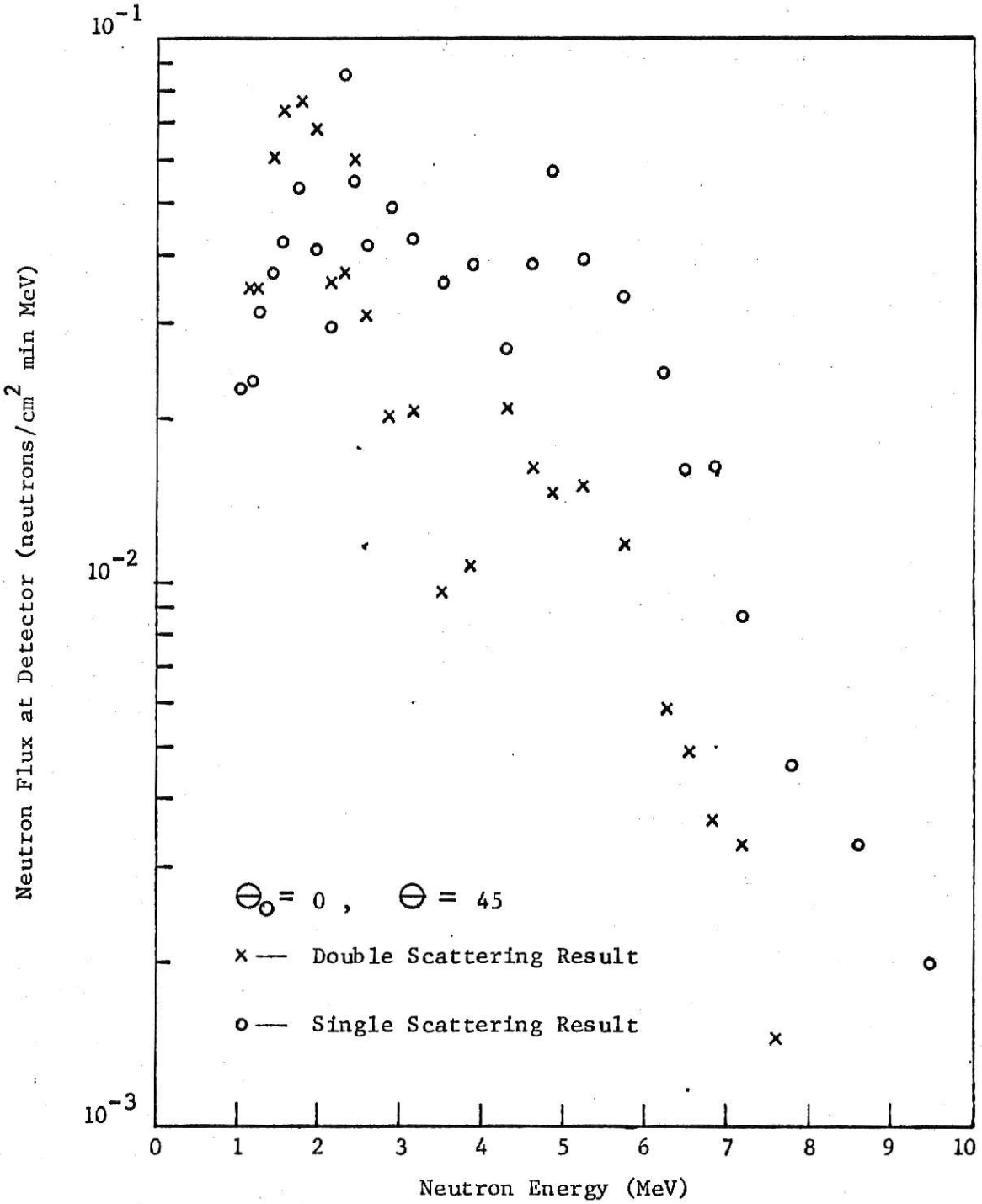

Figure 14. Orders-of-Scattering Calculated Fast-Neutron Penetration Through 22.86 cm. Thick Concrete Slab

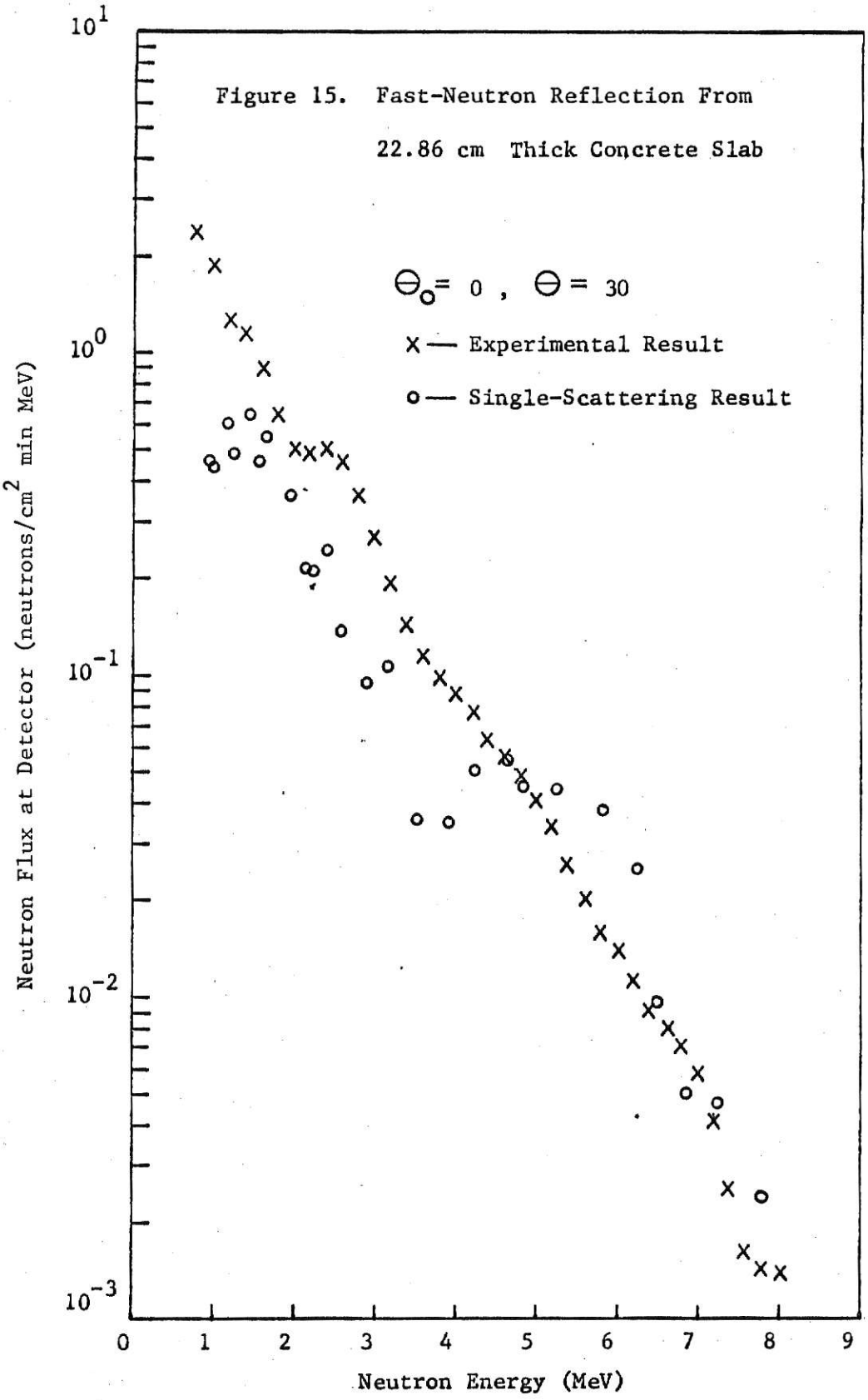
Figure 15. Fast-Neutron Reflection From
22.86 cm Thick Concrete Slab
Θ_o = 0 , Θ = 30
X — Experimental Result
o — Single-Scattering Result
Neutron Flux at Detector (neutrons/cm^2 min MeV)
10^1
10^0
10^{-1}
10^{-2}
10^{-3}
0
1
2
3
4
5
6
7
8
9
Neutron Energy (MeV)

GETIT, was operating properly. Hand calculations were made to duplicate the computational steps that the material synthesis code, MIXUP, executes. The hand calculated results compared to those of the code exactly. This analysis led to the conclusion that errors existed either in the orders-of-scattering codes or in the cross section data.

Single scattering calculations were carried out for water and steel using the DLC-2B cross sections used by Thiesing. The synthesized results of these calculations compared to those made by Thiesing one year ago. This result indicated that the single scattering code was, in fact, working properly.

An intense investigation of the DLC-9 multigroup cross section data was undertaken. Since the DLC-9 cross section set contained hydrogen and oxygen as did the DLC-2B cross section set, the total cross section and 9 Legendre moments of the angular dependent scattering cross section for water were synthesized from the DLC-9 set for comparison with the DLC-2B based water calculations. The angular dependent scattering cross sections for scattering within energy groups and group-to-group were calculated from the 9 Legendre moments of both the DLC-9 and the DLC-2B multigroup cross section sets. Since the cross sections for scattering in-group and group-to-group should be the same in the DLC-9 set as in the DLC-2B set for groups which correspond exactly in energy, the angular dependent scattering cross sections could be compared for several energy groups to reveal differences. Although for water most of the angular dependent scattering cross sections for scattering within an energy group and down to the next lower energy group were comparable for data synthesized from both the DLC-2B and the DLC-9 cross section sets (see Fig. 16-17), the comparison for scattering at particular

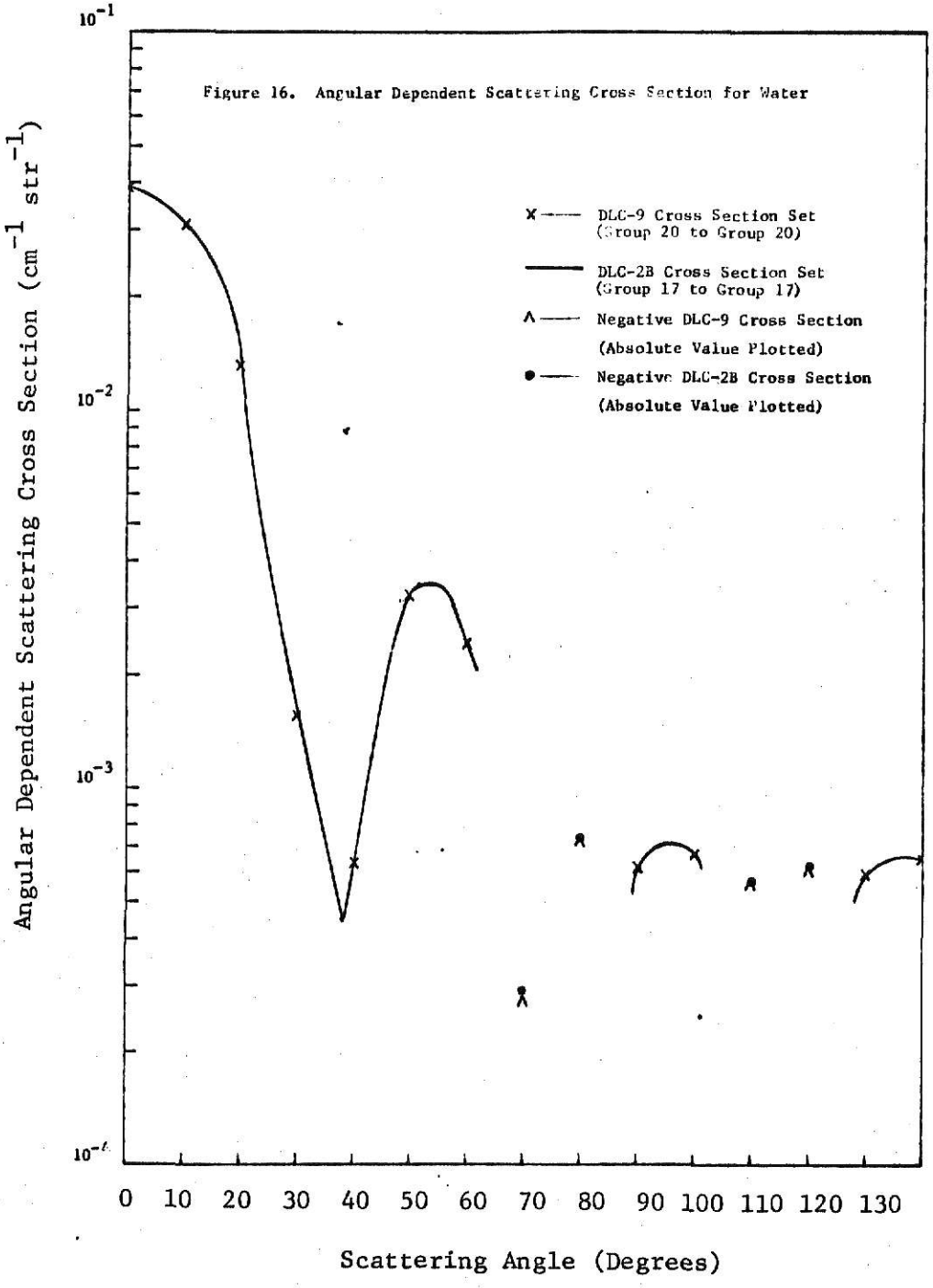
Figure 16. Angular Dependent Scattering Cross Section for Water
DLC-9 Cross Section Set (Group 20 to Group 20)
DLC-2B Cross Section Set (Group 17 to Group 17)
Negative DLC-9 Cross Section (Absolute Value Plotted)
Negative DLC-2B Cross Section (Absolute Value Plotted)
Angular Dependent Scattering Cross Section (cm^{-1} str^{-1})
10^{-1}
10^{-2}
10^{-3}
10^{-4}
0 10 20 30 40 50 60 70 80 90 100 110 120 130
Scattering Angle (Degrees)

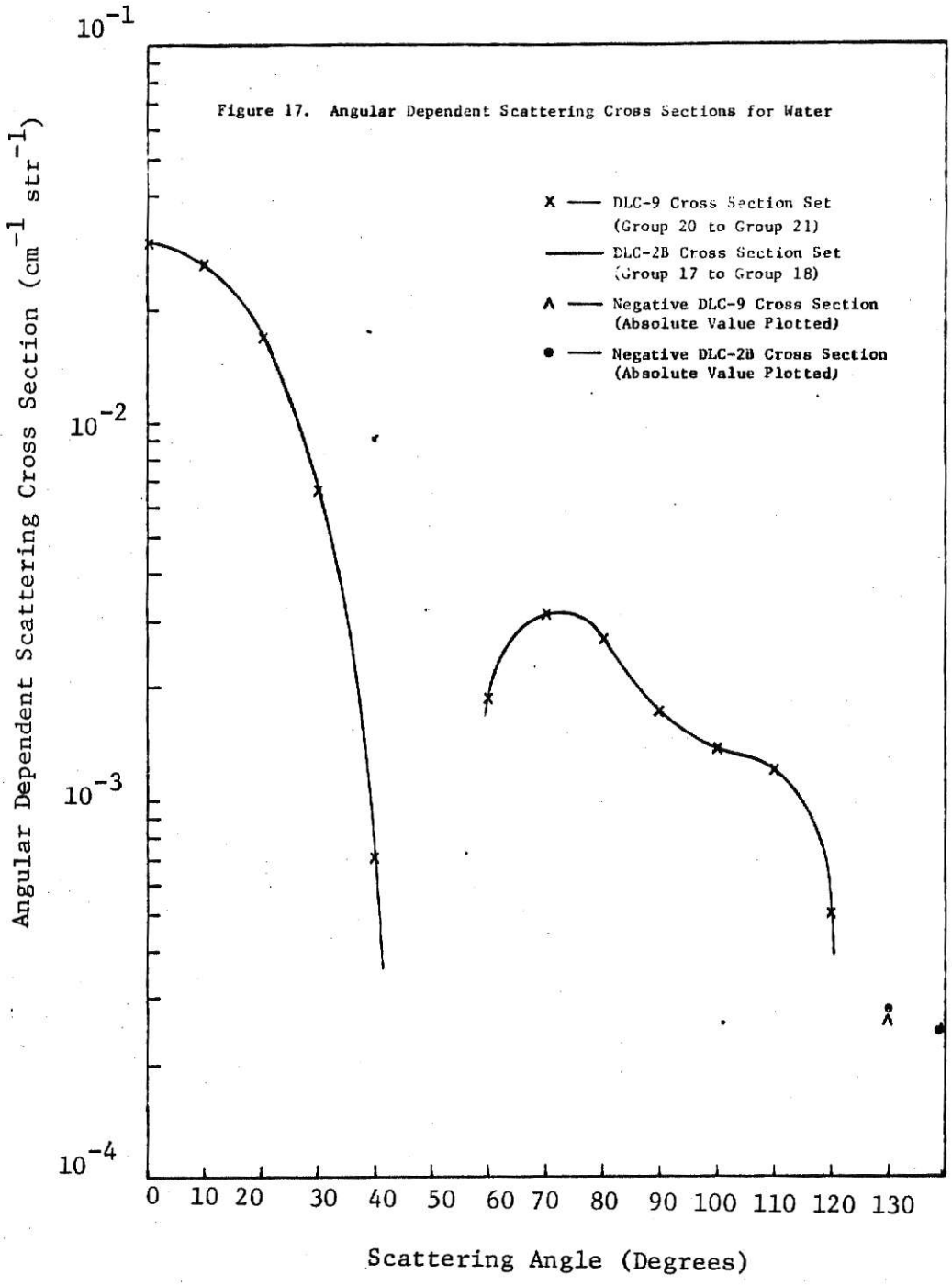
Figure 17. Angular Dependent Scattering Cross Sections for Water
X —— DLC-9 Cross Section Set (Group 20 to Group 21)
—— DLC-2B Cross Section Set (Group 17 to Group 18)
Λ —— Negative DLC-9 Cross Section (Absolute Value Plotted)
● —— Negative DLC-2B Cross Section (Absolute Value Plotted)
Angular Dependent Scattering Cross Section (cm^{-1} str^{-1})
10^{-1}
10^{-2}
10^{-3}
10^{-4}
0 10 20 30 40 50 60 70 80 90 100 110 120 130
Scattering Angle (Degrees)

angles revealed several energy groups where large discrepancies existed (see Fig. 18-21). The reasons for these disagreements in the angular dependent cross sections are assumed to result from the DLC-9 cross section set (the single scattered calculated fast-neutron reflected spectra based on the DLC-2B grouped cross section set compared favorably with the experimental fast-neutron reflection spectra).

Since there was a possibility that the DLC-9 cross section set was generated using a weighting scheme which put more emphasis on forward scattering at the expense of the accuracy of the backscattering cross section values, a 45 degree penetration calculation was performed. Figure 22 shows the synthesized single scattering spectrum for the 45 degree penetration through 20.32 cm of water calculated using the DLC-9 cross section set compared to similar calculations using the DLC-2B cross section set. The DLC-9 based water spectrum for energies above 5 MeV appears to be what would be expected when compared to the DLC-2B spectrum. The errors in the DLC-9 cross sections appear to be in the 1 to 5 MeV energy region and range from 10 to 70%. The water comparison shows that the errors noted were in the DLC-9 generated cross sections and not in the subsequent computations performed with these cross sections.

In an attempt to determine the sensitivity of spectrum calculations to a 10% change in cross section for the single scattering calculation, a 45 degree penetration calculation was performed using the DLC-2B cross sections multiplied by 0.9. Comparison of results between the unaltered calculated spectrum and the altered spectrum are shown in Fig. 23. This comparison shows that the 10% change in the cross section results in a change of about 12% in the calculated neutron spectrum. This deviation is consistent over

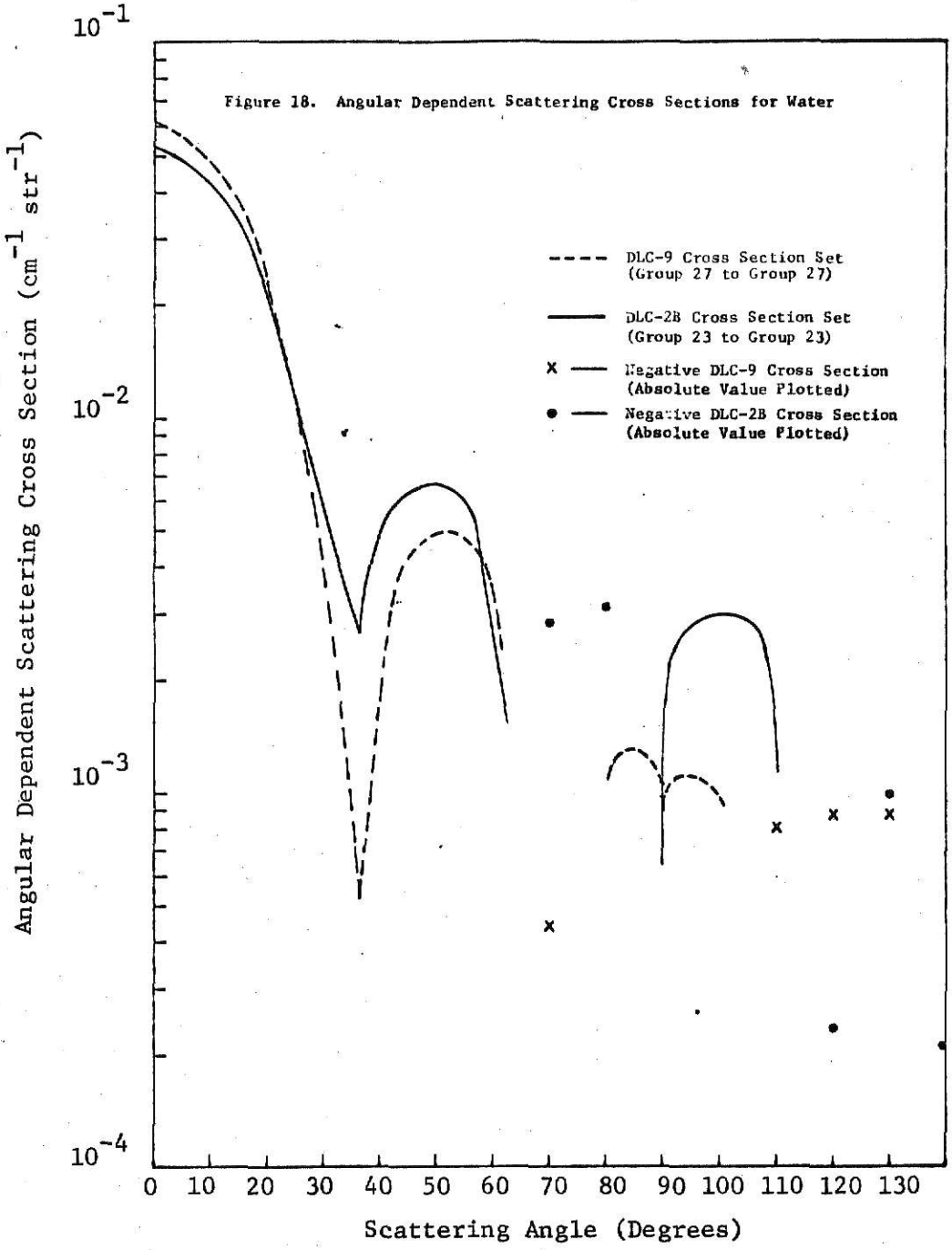
Figure 18. Angular Dependent Scattering Cross Sections for Water
DLC-9 Cross Section Set
(Group 27 to Group 27)
DLC-2B Cross Section Set
(Group 23 to Group 23)
Negative DLC-9 Cross Section
(Absolute Value Plotted)
Negative DLC-2B Cross Section
(Absolute Value Plotted)
Angular Dependent Scattering Cross Section (cm^{-1} str^{-1})
10^{-1}
10^{-2}
10^{-3}
10^{-4}
0 10 20 30 40 50 60 70 80 90 100 110 120 130
Scattering Angle (Degrees)

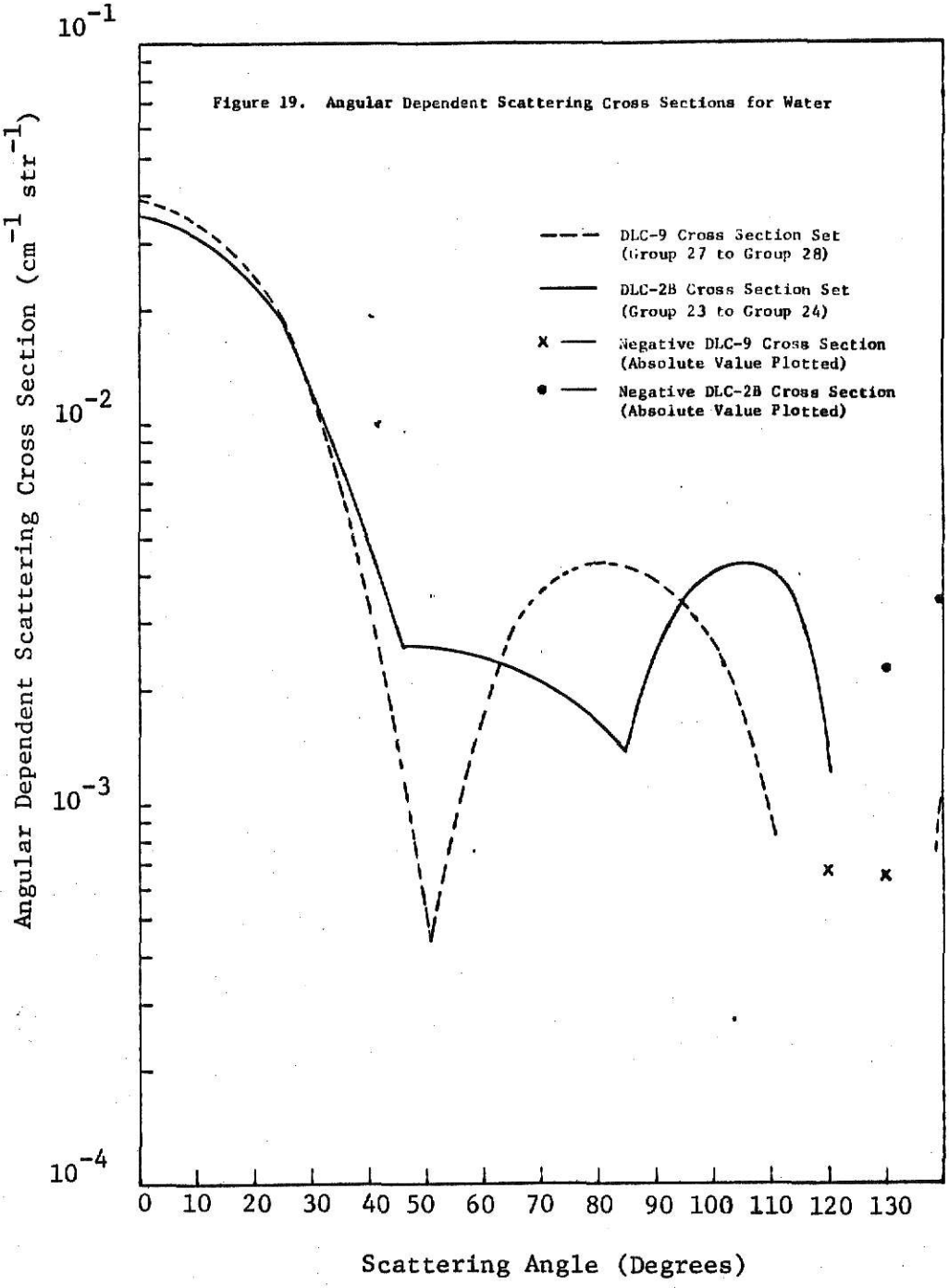
Figure 19. Angular Dependent Scattering Cross Sections for Water
DLC-9 Cross Section Set
(Group 27 to Group 28)
DLC-2B Cross Section Set
(Group 23 to Group 24)
Negative DLC-9 Cross Section
(Absolute Value Plotted)
Negative DLC-2B Cross Section
(Absolute Value Plotted)
Angular Dependent Scattering Cross Section (cm^{-1} str^{-1})
10^{-1}
10^{-2}
10^{-3}
10^{-4}
0 10 20 30 40 50 60 70 80 90 100 110 120 130
Scattering Angle (Degrees)

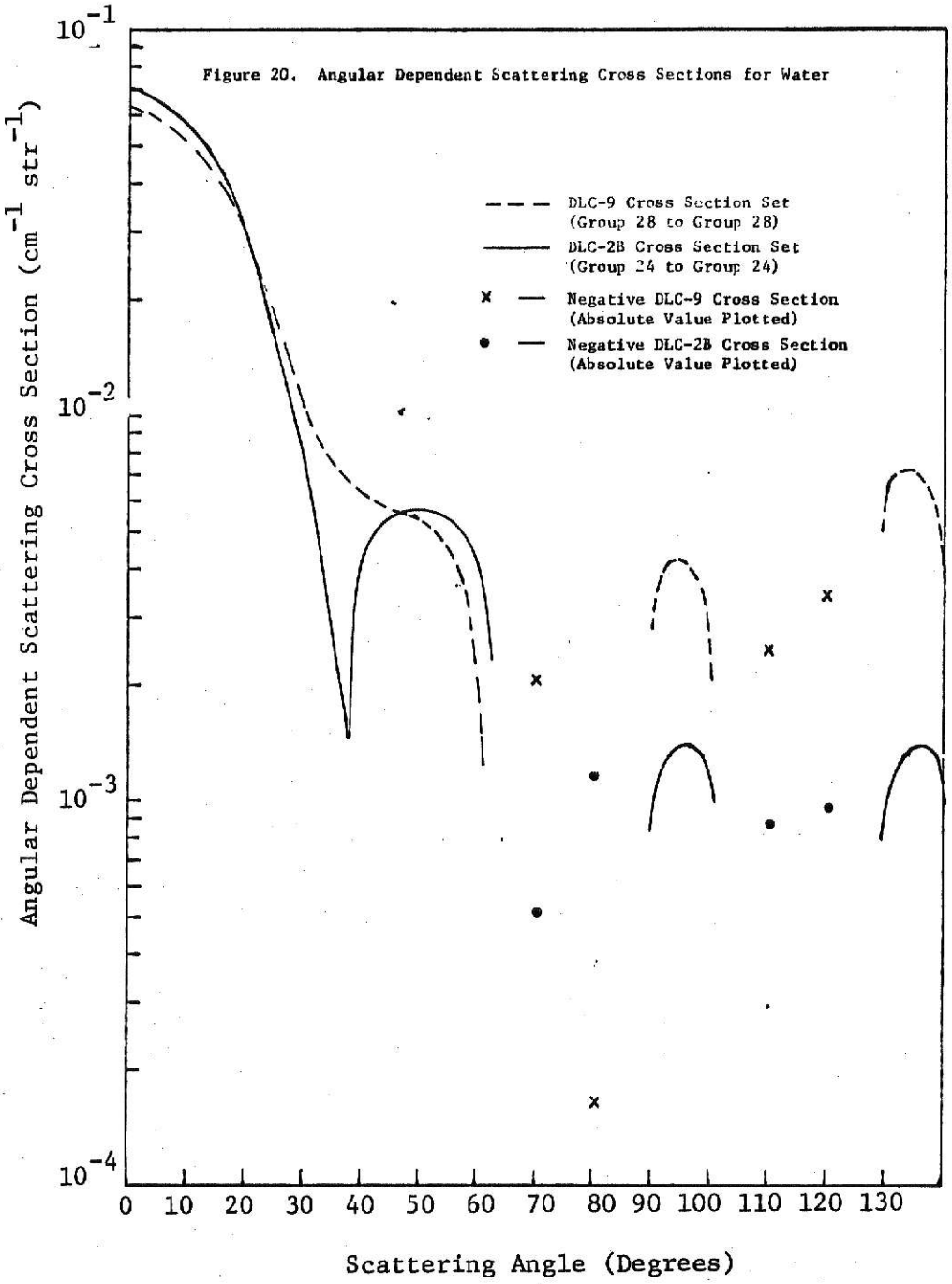
Figure 20. Angular Dependent Scattering Cross Sections for Water
DLC-9 Cross Section Set
(Group 28 to Group 28)
DLC-2B Cross Section Set
(Group 24 to Group 24)
Negative DLC-9 Cross Section
(Absolute Value Plotted)
Negative DLC-2B Cross Section
(Absolute Value Plotted)
Angular Dependent Scattering Cross Section (cm^{-1} str^{-1})
10^{-1}
10^{-2}
10^{-3}
10^{-4}
0 10 20 30 40 50 60 70 80 90 100 110 120 130
Scattering Angle (Degrees)

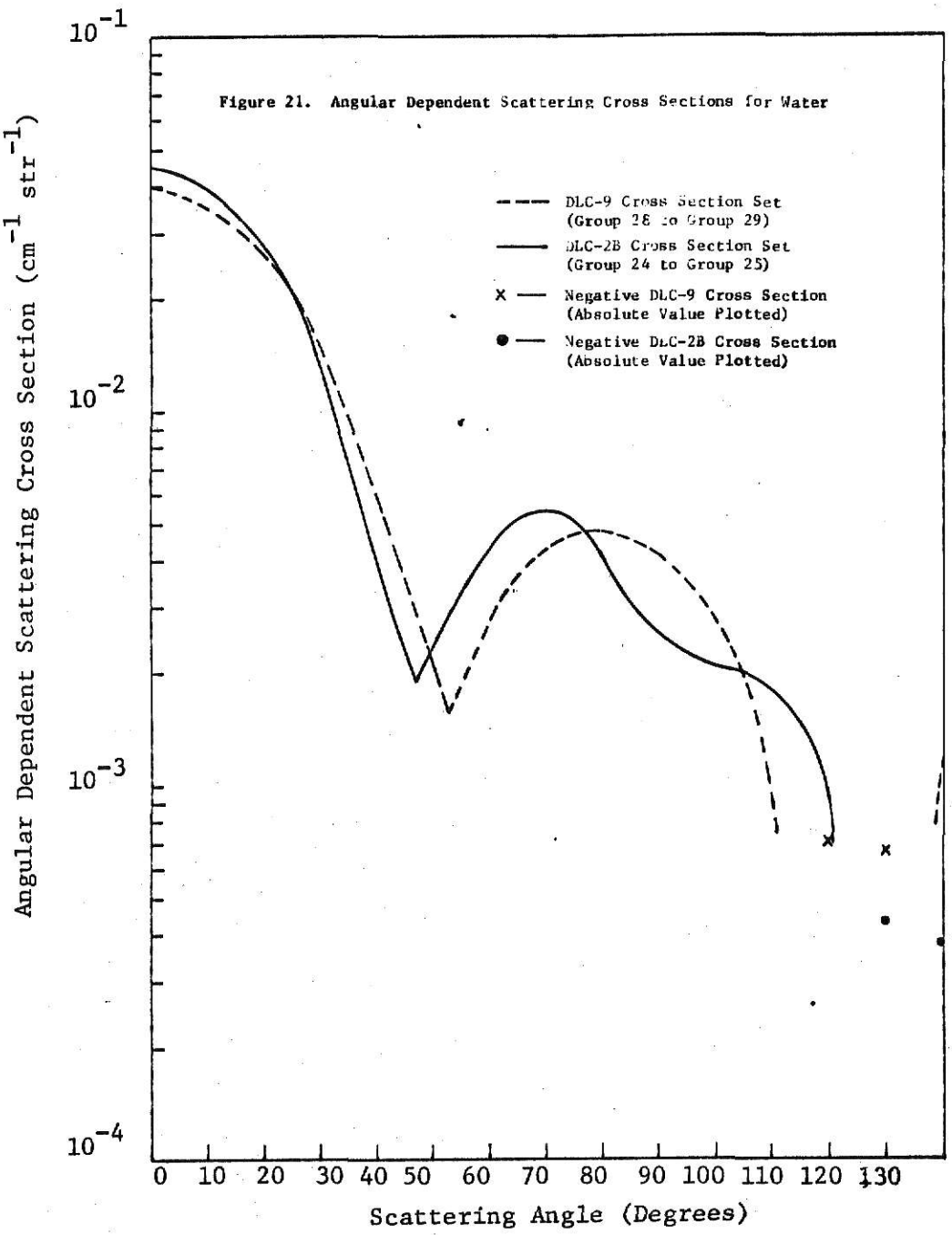
Figure 21. Angular Dependent Scattering Cross Sections for Water
DLC-9 Cross Section Set
(Group 28 to Group 29)
DLC-2B Cross Section Set
(Group 24 to Group 25)
Negative DLC-9 Cross Section
(Absolute Value Plotted)
Negative DLC-2B Cross Section
(Absolute Value Plotted)
Angular Dependent Scattering Cross Section (cm^{-1} str^{-1})
10^{-1}
10^{-2}
10^{-3}
10^{-4}
0 10 20 30 40 50 60 70 80 90 100 110 120 130
Scattering Angle (Degrees)

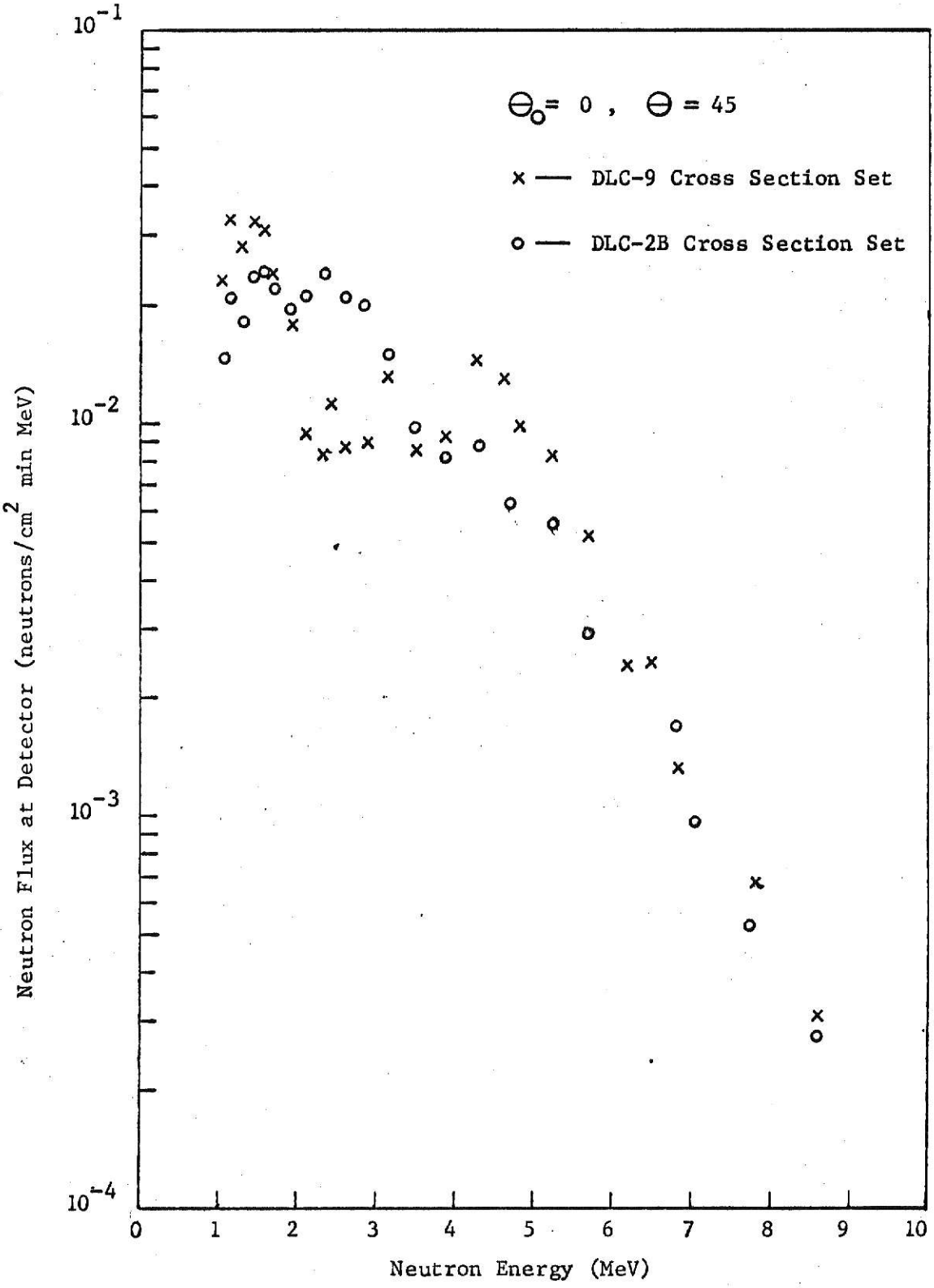

Figure 22. Single Scatter Calculated Fast-Neutron Penetration Through 20.32 cm Thick Water Slab

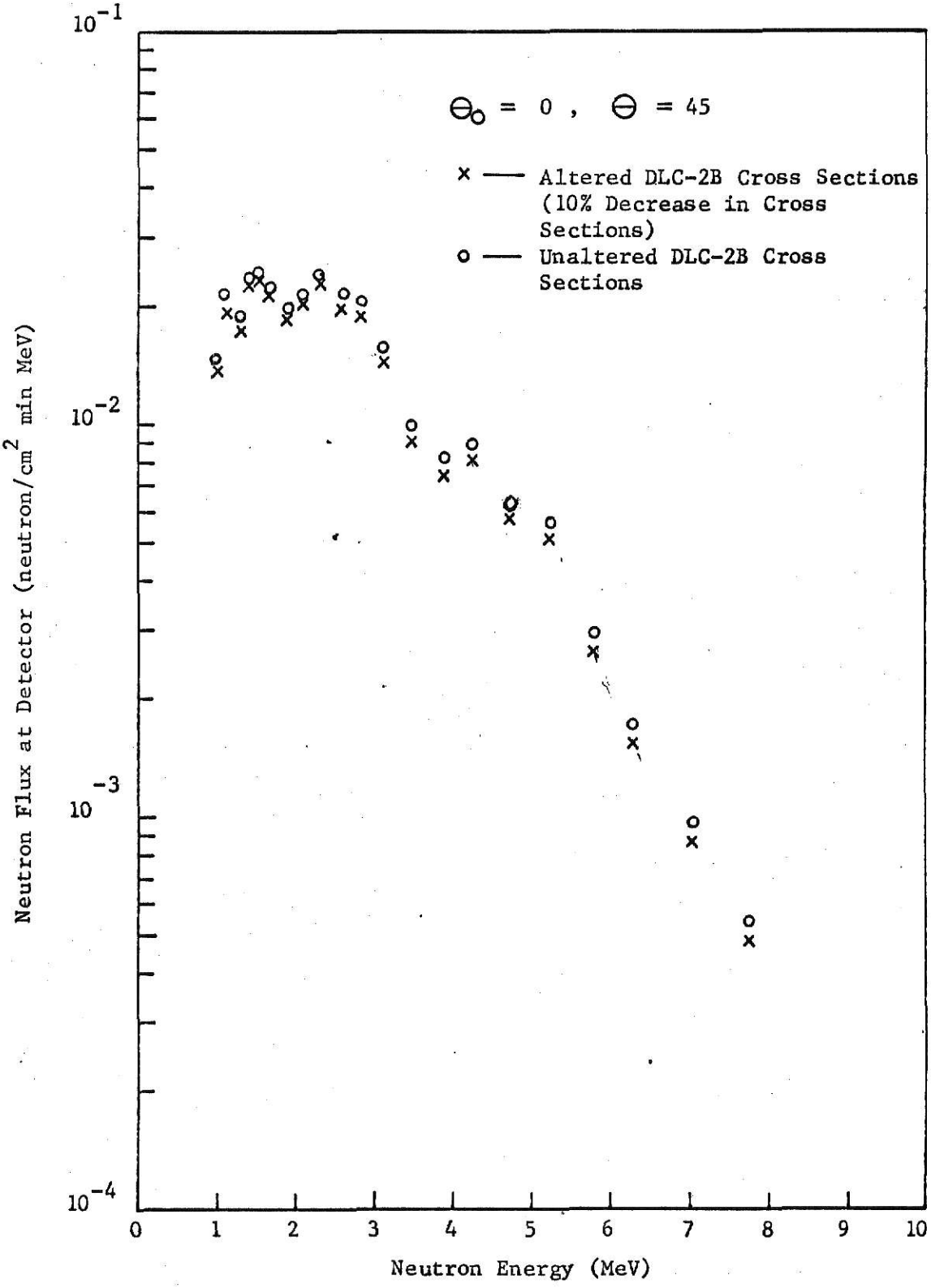

Figure 23. Single Scatter Calculated Fast-Neutron Penetration Through 20.32 cm Thick Water Slab

the entire energy range of 1 to 8 MeV. By comparing this result with the results of Fig. 22 it is estimated that the DLC-9 cross section set differs from the DLC-2B cross sections by 10 to 65%.

6.0 SUGGESTIONS FOR FURTHER STUDY

The principal objectives of this work were to measure neutron spectra reflected from thick slabs of concrete and steel and to determine the angular and energy dependent dose albedos for these two important shielding materials. In addition, the experimental fast-neutron spectra were compared with orders-of-scattering and Monte Carlo calculations.

Further experiments need to be undertaken to study the reflection of fast-neutrons from water as well as the penetration of fast-neutrons through all three principal shielding materials, steel, concrete and water. In depth calculations need to be performed using the latest updated cross section information to verify the experimental results.

Since the DLC-9 cross section set used in this work appeared to contain errors, an investigation into this set is required to determine the source of these errors. Were they just in the particular tape used, in the multigroup cross section compilation codes, SUPERTOG, or in the ENDF/B point cross section library? Also, a study of the effects of small differences in cross sections on the orders-of-scattering codes should be studied in more depth.

7.0 ACKNOWLEDGEMENTS

The author wishes to express his sincerest gratitude to Dr. Walter Meyer for all of his help and advice throughout the course of this study. Special thanks must be extended to the Department of Nuclear Engineering for the financial assistance and to the faculty and staff for their repeated encouragement to continue. Also, a special note of thanks is extended to J. W. Thiesing and T. R. Hill for their assistance in understanding the multi-group cross section sets and other related material. Finally, extra special thanks with love are given to my wife, Ronda, and to Spasy for their encouragement and support.

8.0 REFERENCES

1. F. J. Allen, A. Futterer, W. Wright, "Neutron Reflections Flux versus Depth for Water, Aluminum, Iron, and Concrete," BRL Report No.s 1204, 1238, 1199, 1189 (1963).

2. R. E. Maerker and F. J. Muckenthaler, "Differential Fast-Neutron Albedos for Concrete," ORNL-2822, Vols. I-VI (October, 1965).

3. W. Meyer, D. H. Timmons, P. K. Shen, "One Dimensional S_n Calculations of Neutron Spectra Reflected from Thick Slabs of Concrete and Iron, Comparison with Experiment," AEC Document COOo-2049-2 (1970).

4. R. Bednarz and A. Kuzzell, "Semi-infinite Albedo Problem," Institute of Nuclear Research, Warsaw (1968).

5. Y. T. Song, "Semi-Empirical Formula for Differential Dose Albedo for Fast-Neutrons on Various Materials," Trans. Am. Nuc. Soc., 10:727-8 (November 1967).

6. B. J. Henderson, "Conversion of Neutron or Gamma Ray Flux to Absorbed Dose Rate," XDC-59-8-179 (159).

7. W. R. Burrus, "Utilization of A Priori Information in the Statistical Interpretation of Measured Distributions," ORNL-3742 (1964).

8. J. W. Thiesing and W. Meyer, "The Orders-of-Scattering Method for Fast-Neutron Transport," AEC Document No. COO-2049-9 (August 25, 1971).

9. DLC-2B, 99 Group Cross Sections, Radiation Shielding Information Center, Oak Ridge National Laboratory 1969.

10. DLC-9, 122 Group Neutron and Gamma Ray Cross Sections, Radiation Shielding Information Center, Oak Ridge National Laboratory, 1972.

11. H. C. Honeck, "ENDF/B, Specifications for an Evaluated Nuclear Data File for Reactor Applications," BNL-5066, T-467 (1966).

12. R. Q. Wright, J. L. Lucius, N. M. Greene and C. W. Craven, "SUPERTOG: A Program to Generate Fine Group Constants and P_n Scattering Matrices from ENDF/B," ORNL-TM-2679 (1969).

13. V. V. Verbinski, "Calibration of an Organic Scintillator for Neutron Spectroscopy," ORNL-TM 2183 (June 10, 1968).

14. W. Meyer, J. W. Thiesing and C. M. Estimes, "Intercalibration of the Kansas State University NE-213 Fast-Neutron Spectrometer," AEC Document COO-2049-2 (December 1970).

15. W. Meyer and W. H. Miller, "Evaluation of Minima in Total Neutron Cross Sections by Transmissions of Fission Spectra Through Thick Samples," AEC Document No. COO-2049-5 (July 30, 1971).

16. W. H. Miller and W. Meyer, "Experimental Evaluation of Minimum and Shallow-Angle-Scattering Neutron Cross Sections," Trans. Am. Nuc. Soc., 14, 902 (1971).

17. G. G. Simons, "Development, Calibration and Utilization of the KSU NE-213 Fast-Neutron Spectrometer," Ph.D. Dissertation, Kansas State University, Manhattan, Kansas (1969).

18. C. E. Clifford, E. A. Straker, F. J. Muckenthaler, V. V. Verbinski, R. M. Freestone, Jr., K. M. Henry and W. R. Burrus, "Measurements of the Spectra of Uncollided Fission Neutrons Transmitted Through Thick Samples of Nitrogen, Oxygen, Carbon and Lead: Investigation of the Minima in Total Cross Sections," Nuc. Sci. and Eng., 27, 299-307 (1967).

9.0 APPENDICES

APPENDIX A

Cross Section Transformation Code, GETIT

The cross section transformation code, GETIT, extracts the total cross sections and 9 Legendre moments of the group-to-group angular dependent scattering cross section from the DLC-2 or DLC-9 magnetic tape then transforms them into the appropriate form and writes them onto another tape. The subroutine, BOWWOW, written and documented by T. R. Hill of the Nuclear Engineering Department at Kansas State, is used to read the input cross sections. The operation of this code can be described by the following user's guide:

CARD	FORMAT	
1	16I5	1. NELEM - Number of elements to be read from the tape. 2. NORDR - Order of the Legendre Expansion used to express the angular dependent scattering cross sections (9). 3. NGPO - Number of groups to be transferred to the DLC-9 tape (34).

ILLEGIBLE DOCUMENT

THE FOLLOWING DOCUMENT(S) IS OF POOR LEGIBILITY IN THE ORIGINAL

THIS IS THE BEST COPY AVAILABLE

GETIT Listing

```
C     ******************************************************************
C     THIS CODE TAKES THE FIRST 'NGPO' NEUTRON GROUPS OFF OF THE DLC-9
C     TAPE AND MAKES ANOTHER TAPE
C     THIS CODE MAKES USE OF THE SUBROUTINE 'BOWWOW'
C     ******************************************************************
      DIMENSION SIGA(122), VSIGF(122), SIGT(122), SIGSCT(122,122)
    1 FORMAT(16I5)
    2 FORMAT(37X,I4,7X,I3,14X,I1)
    3 FORMAT(1X,15HMATERIAL NUMBER,I5,2X,I4,1X,6HGROUPS,2X,I2,1X,5HORDER
     1)
    4 FORMAT(1X,5E14.6)
      READ(1,1) NELEM, NORDR , NGPO
      DO 100 IELEM=1,NELEM
      DO 100 IORD=1,NORDR
      READ(8,2) MATNO, NGPS, NORD
      CALL BOWWOW(NGPS,SIGA,VSIGF,SIGT,SIGSCT,122)
      WRITE(3,3)MATNO,NGPO,IORD
      WRITE(9,3) MATNO,NGPO,IORD
      IF(IORD.GT.1) GO TO 99
      WRITE(3,4) (SIGA(I),I=1,NGPO)
      WRITE(9,4) (SIGA(I),I=1,NGPO)
      WRITE(3,4) (SIGT(I),I=1,NGPO)
      WRITE(9,4) (SIGT(I),I=1,NGPO)
   99 DO 98 J=1,NGPO
      WRITE(3,4) (SIGSCT(I,J),I=1,NGPO)
   98 WRITE(9,4) (SIGSCT(I,J),I=1,NGPO)
  100 CONTINUE
      STOP
      END
      SUBROUTINE BOWWOW(NGPS,SIGA,VSIGF,SIGT,SIGSCT,MAXG)
C**** TOM HILL VERSION OF ANISN INPUT SUBROUTINE--> FIDO
C        THIS VERSION DOES NOT KEY ON THE ICARD PARAMETER
      DIMENSION SIGA(MAXG),VSIGF(MAXG),SIGT(MAXG),SIGSCT(MAXG,MAXG)
      DIMENSION NUM(6),FLAG(6),VALU(6)
      LOGICAL*1 NEWGP
    1 FORMAT(6(I2,A1,E9.0),4X,I4)
      DATA R/'R'/
      DO 9 I=1,NGPS
      SIGA(I)=0.
      VSIGF(I)=0.
      SIGT(I)=0.
      DO 9 J=1,NGPS
    9 SIGSCT(I,J)=0.
      IGP=1
      NEWGP=.TRUE.
C**** READ NEW DATA CARD
   10 READ(8,1) (NUM(I),FLAG(I),VALU(I),I=1,6),ICARD
C**** IS THIS A SECONDARY CARD???   KEY SWITCH ON NEWGP PARAMETER
      IF(.NOT.NEWGP) GO TO 50
C**** NAY, IT'S A PRIMARY CARD FOR THE NEW  GROUP
```

```
C**** SET ABSORPTION CROSS SECTION
      SIGA(IGP)=VALU(1)
C**** SET FISSION CROSS SECTION
      VSIGF(IGP)=VALU(2)
      IF((NUM(1).GT.1).AND.(FLAG(1).EQ.R)) VSIGF(IGP)=VALU(1)
C**** SET TOTAL CROSS SECTION
      SIGT(IGP)=VALU(3)
      IF((NUM(1).GT.2).AND.(FLAG(1).EQ.R)) SIGT(IGP)=VALU(1)
      IF((NUM(1).EQ.2).AND.(FLAG(1).EQ.R)) SIGT(IGP)=VALU(2)
      IF((NUM(2).GT.1).AND.(FLAG(2).EQ.R)) SIGT(IGP)=VALU(2)
C**** LOCATE POSITION OF DIAGONAL ELEMENT ON CARD
      IPOS=4
      IF((NUM(1).GT.3).AND.(FLAG(1).EQ.R)) IPOS=1
      IF((NUM(1).EQ.3).AND.(FLAG(1).EQ.R)) IPOS=2
      IF((NUM(1).EQ.2).AND.(FLAG(1).EQ.R)) IPOS=3
      IF((NUM(2).GT.2).AND.(FLAG(2).EQ.R)) IPOS=2
      IF((NUM(2).EQ.2).AND.(FLAG(2).EQ.R)) IPOS=3
C**** POSITION OF SELF-SCATTER ELEMENT IS IN IPOS
      SIGSCT(IGP,IGP)=VALU(IPOS)
C**** NOW START COUNT ON SCATTERING MATRIX COLUMN
      ICOL=IGP-1
      NEWGP=.FALSE.
      ICOUNT=NGPS-1
C**** ICOUNT=0 MEANS THIS GROUP HAS BEEN FILLED
      IPOS=IPOS+1
      DO 20 I=IPOS,6
      NREP=1
      IF(FLAG(I).EQ.R) NREP=NUM(I)
      IF(ICOUNT.EQ.0) GO TO 100
      DO 20 J=1,NREP
      IF(ICOL.EQ.0) GO TO 20
      SIGSCT(IGP,ICOL)=VALU(I)
      ICOL=ICOL-1
   20 ICOUNT=ICOUNT-1
      IF(ICOUNT.LE.0) GO TO 100
C**** GO BACK AND READ A SECONDARY CARD
      GO TO 10
C**** THIS IS A SECONDARY CARD WITH KERNEL ONLY
   50 CONTINUE
      DO 60 I=1,6
      NREP=1
      IF(FLAG(I).EQ.R) NREP=NUM(I)
      IF(ICOUNT.EQ.0) GO TO 100
      DO 60 J=1,NREP
      IF(ICOL.EQ.0) GO TO 60
      SIGSCT(IGP,ICOL)=VALU(I)
      ICOL=ICOL-1
   60 ICOUNT=ICOUNT-1
      IF(ICOUNT.LE.0) GO TO 100
C**** GO BACK AND READ ANOTHER SECONDARY CARD
      GO TO 10
C**** KERNEL FOR GROUP COMPLETED, START NEW GROUP
```

```
  100 IGP=IGP+1
      IF(IGP.GT.NGPS) RETURN
      NEWGP=.TRUE.
C**** GO BACK AND READ NEW PRIMARY CARD
      GO TO 10
      END
```

APPENDIX B

Multi-Component Material Synthesis Code, MIXUP

The multi-component material synthesis code, MIXUP, multiplies the DLC-9 or DLC-2 total cross sections and 9 Legendre moments of the angular dependent cross sections for the component nuclides by the appropriate number densities, adds them up and writes the resultant total cross sections and Legendre moments on paper, cards and/or tape. The input to this code includes the output, tape or cards, of the code, GETIT. The operation of the code that performs this operation is described by the following user's guide:

CARD	FORMAT	
1	1615	1. NELEM - Number of nuclides on the input tape. 2. NORDR - 1 + Legendre expansion order (9). 3. NGPO - Number of groups to be transferred to the DLC-9 tape (34).
2	8F10.0	AND(I), I=1,NELEM - Nuclear density (x 10^{-24}) for the nuclides, in order, on the input tape. (If a nuclide is not in mixture, AND(I)=0).

Output will be a tape or cards containing:

Blank card
Total cross sections
2 blank cards
P_o scattering matrix
2 blank cards
P_1 scattering matrix
etc.

MIXUP Listing

```
C     ****************************************************************
C     THIS CODE MULTIPLIES THE CROSSSECTIONS BY THE PROPER NUCLEAR
C     DENSITIES, ADDS THEM UP, AND MAKES ANOTHER TAPE AND/OR CARDS
C      SUITABLE FOR INPUT TO THE ORDERS-OF-SCATTERING CODES
C     ****************************************************************
      DIMENSION T(20),SIGA(34),SIGT(34),SIGSCT(34,34,9),AND(10),SIA(34)
      DIMENSION SIT(34),SISCT(34,34,9)
    1 FORMAT (1615)
    2 FORMAT (8E10.3)
    3 FORMAT (1X,5E14.6)
    4 FORMAT (20A4)
    5 FORMAT(80X)
      READ(1,1) NELEM, NORDR, NGPC
      DO 10 I=1,NGPC
      SIA(I)=0.
      SIT(I)=0.
      DO 10 J=1,NGPC
      DO 10 IORDR=1,NORDR
   10 SISCT(I,J,IORDR)=0.
      READ(1,2) (AND(I), I=1,NELEM)
      DO 400 IELEM=1,NELEM
      DO 100 IORDR=1,NORDR
      READ(8,4) (T(I),I=1,20)
      IF(IORDR.GT.1) GO TO 97
      READ(8,3) (SIGA(I), I=1,NGPC)
      READ(8,3) (SIGT(I), I=1,NGPC)
   97 CONTINUE
      DO 98 I=1,NGPC
   98 READ(8,3) (SIGSCT(I,J,IORDR), J=1,NGPC)
  100 CONTINUE
      DO 96 I=1,NGPC
   96 SIT(I)=SIT(I)+SIGT(I)*AND(IELEM)
      DO 95 IORDR=1,NORDR
      DO 95 I=1,NGPC
      DO 95 J=1,NGPC
   95 SISCT(I,J,IORDR)=SISCT(I,J,IORDR)+SIGSCT(I,J,IORDR)*AND(IELEM)
  400 CONTINUE
      WRITE(3,5)
      WRITE(2,5)
      WRITE(2,3) (SIT(I),I=1,NGPC)
      WRITE(3,3) (SIT(I), I=1,NGPC)
      DO 94 IORDR=1,NORDR
      WRITE(2,5)
      WRITE(2,5)
      WRITE(3,5)
      WRITE(3,5)
      DO 94 I=1,NGPC
      WRITE(2,3) (SISCT(I,J,IORDR),J=1,NGPC)
   94 WRITE(3,3)(SISCT(I,J,IORDR), J=1,NGPC)
      STOP
      END
```

APPENDIX C

Experimental Albedo Determination Code, ALBEE

The experimental dose albedo determination code, ALBEE, calculates the dose albedos from the experimental fast-neutron reflection spectra, the direct neutron beam spectrum, nickel foil fluence numbers and slab to detector radius. In addition, the dose albedos are determined from the Monte Carlo calculated double differential dose albedos. The operation of this code can be described by the following user's guide:

CARD	FORMAT	
1	F10.0, E13.6, F10.0, E13.6	1. EO(I),I=1,5 - Energy corresponding to the midpoint of the Monte Carlo data energy bins. 2. YD(I) - ORNL double differential dose albedos. 3. DELEO(I) - Width of the i^{th} ORNL energy bin. 4. C(I) - Henderson's flux-to-dose conversion factor corresponding to energy EO(I).
2	F10.0, E13.6, F10.0, E13.6	1. EE(I),I=1,32 - Energy corresponding to the i^{th} energy group of the DLC-9 cross section set. 2. YDB(I),I=1,32 - Number of neutrons in direct beam at energy EE(I). 3. DELEO(I),I=1,32 - Width of the i^{th} energy group of the DLC-9 cross section set. 4. CE(I),I=1,32 - Henderson's flux-to-dose conversion factor corresponding to the energy EE(I).
3 deck	8E10.3	CP(JK)JK=1,48 - Henderson's flux-to-dose conversion factors corresponding to the FERDOR energy bins.
4	4X,E12.5	FLUDB - Direct beam fluence from Nickel foil data.
5	16I5	NDS - Number of data sets.

6	16I5	IDENT - Identification number (1 if Monte Carlo data is available for comparison; otherwise 0).
7	20A4	TITLE(I),I=1,20 - Arbitrary title card for Monte Carlo data.
8 deck	10X,5F7.5	DD(J,JK),J=1,5,JK=1,7 - Monte Carlo calculated double differential dose albedos.
9	4X,E12.5	FLUREF - Reflection fluence from nickel foil data.
10	20A4	TITLE(I),I=1,20 - Arbitrary title code for experimental reflection spectra.
11 deck	8X,E10.3, 3X,E10.3	1. E(J),J=1,105 - Energy values from FERDOR unfolding code. 2. Y(J),J=1,105 - Unfolded neutron spectra corresponding to energies E(J).

The first 5 cards are entered only once. If there are no Monte Carlo data to compare with the experimental data, cards 7-8 are omitted and card 6 has the value zero. Cards 9-11 are entered for each experimental spectrum analyzed.

ALBEE Listing

```
      DIMENSION EO(7),DELEO(7),C(7),YD(7),EE(32),DELEE(32),CE(32),
     1DEN(32),DD(5,7),TITLE(20),DNUM(5),DOSE(50),CNUM(48),IBUF(1000),
     2YY(52),E(105),Y(105),YDB(32),CP(50)
    1 FORMAT(F10.0,E13.6,F10.0,E10.3)
    2 FORMAT(8X,E10.3,3X,E10.3)
    3 FORMAT(5X,I5,3X,E12.3)
    4 FORMAT(4X,E12.5)
    5 FORMAT(10X,5F7.5)
    6 FORMAT(20A4)
    7 FORMAT(8E10.3)
   16 FORMAT(16I5)
      NREAD=5
      NPRINT=6
      NPUNCH=7
      DO 8 I=1,5
    8 READ(NREAD,1) EO(I),YD(I),DELEO(I),C(I)
      DO 9 I=1,32
    9 READ(NREAD,1) EE(I),YDB(I),DELEE(I),CE(I)
      READ(NREAD,7)(CP(JK),JK=1,48)
      READ(NREAD,4) FLUDB
      RAD=167.64
C     CALCULATION OF THE ORNL DOSE ALBEDO
      DENT=0.0
      DO 10 I=1,32
      DEN(I)=DELEE(I)*YDB(I)*CE(I)
   10 DENT=DENT+DEN(I)
      READ(NREAD,16)NDS
      DO 32 MM=1,NDS
      READ(NREAD,16)IDENT
      IF(IDENT.EQ.0)GO TO 17
      READ(NREAD,6)(TITLE(II),II=1,20)
      WRITE(NPRINT,6) TITLE
      DO 14 JK=1,7
   14 READ(NREAD,5)(DD(J,JK),J=1,5)
      DO 12 JK=1,7
      SNUM=0.0
      DO 11 J=1,5
      DNUM(J)=DELEO(J)*YD(J)*C(J)*DD(J,JK)
   11 SNUM=SNUM+DNUM(J)
      DOSE(JK)=SNUM/DENT
      WRITE(NPRINT,3)JK,DOSE(JK)
   12 CONTINUE
   17 CONTINUE
C     CALCULATION OF CORRESPONDING KSU DOSE ALBEDO
      READ(NREAD,4) FLUREF
      READ(NREAD,6)(TITLE(II),II=1,20)
      WRITE(NPRINT,6) TITLE
      DENTE=DENT*1.0/(RAD**2.0)
      DO 13 J=1,105
   13 READ(NREAD,2) E(J),Y(J)
```

```
      DO 15 M=1,48
      CNUM(M)=Y(M)*CP(M)*FLUDB/FLUREF
      DOSE(M)=CNUM(M)/DENTE
      WRITE(NPRINT,3) M,DOSE(M)
   15 CONTINUE
      STOP
      END
```

ALBEE Input Data

```
   1.125 0.804848E 06       0.75 0.862E-05
    2.25 0.508479E 06        1.5 0.113E-04
     3.5 0.222685E 06          1 0.148E-04
     5.0 0.111878E 06          2 0.152E-04
     7.0 0.374954E 05          2 0.162E-04
 0.95488 0.598723E 06    0.09541 0.800E-05
 1.05531 0.715882E 06    0.10544 0.863E-05
 1.16628 0.857167E 06    0.11653 0.885E-05
 1.28895 0.885825E 06    0.12879 0.944E-05
 1.42452 0.857925E 06    0.14234 0.939E-05
 1.57434 0.821515E 06    0.15730 0.995E-05
 1.73991 0.790965E 06    0.17384 0.102E-04
 1.92289 0.692877E 06    0.19213 0.109E-04
 2.12513 0.547363E 06    0.21234 0.115E-04
 2.29065 0.495725E 06    0.11870 0.114E-04
 2.40798 0.462307E 06    0.11597 0.112E-04
 2.59564 0.413311E 06    0.25935 0.120E-04
 2.86863 0.357052E 06    0.28662 0.128E-04
 3.17082 0.283813E 06    0.31677 0.136E-04
 3.50375 0.221944E 06    0.35008 0.148E-04
 3.87224 0.191143E 06    0.38691 0.152E-04
 4.27949 0.168376E 06    0.42751 0.163E-04
 4.62164 0.138690E 06    0.25671 0.151E-04
 4.85792 0.121049E 06    0.21585 0.156E-04
 5.22698 0.972175E 05    0.52227 0.156E-04
 5.77667 0.767894E 05    0.57219 0.161E-04
 6.21265 0.633430E 05    0.29469 0.164E-04
 6.53160 0.531742E 05    0.34320 0.163E-04
 6.85160 0.425562E 05    0.29680 0.163E-04
 7.20409 0.335713E 05    0.40818 0.165E-04
 7.79774 0.246725E 05    0.77913 0.176E-04
 8.61783 0.135336E 05    0.86106 0.175E-04
 9.52460 0.711631E 04    0.95160 0.173E-04
10.52580 0.261667E 04    1.05170 0.183E-04
11.63280 0.482503E 03    1.16233 0.190E-04
12.85630 0.767808E 03    1.28460 0.197E-04
14.24930 0.563924E 03    1.50140 0.196E-04
0.707E-05 0.773E-05 0.872E-05 0.854E-05 0.885E-05 0.944E-05 0.939E-05 0.968E-05
0.595E-05 0.102E-04 0.107E-04 0.109E-04 0.108E-04 0.115E-04 0.112E-04 0.114E-04
0.112E-04 0.118E-04 0.120E-04 0.121E-04 0.124E-04 0.128E-04 0.127E-04 0.142E-04
0.145E-04 0.151E-04 0.160E-04 0.149E-04 0.153E-04 0.163E-04 0.154E-04 0.156E-04
0.161E-04 0.156E-04 0.157E-04 0.160E-04 0.161E-04 0.162E-04 0.164E-04 0.164E-04
0.163E-04 0.163E-04 0.162E-04 0.165E-04 0.170E-04 0.175E-04 0.176E-04 0.171E-04
  0.36477E 02
 1
 1
 *** ORNL ALBEDO VALUES   THETAD=60 , THETA=128 , PHI=135 ***
.8-1.0  0.150000.015800.007300.005780.00480
1.-1.5  0.036800.043900.009540.005250.00491
1.5-2.  0.0     0.041600.010200.006220.00378
```

```
2.-3.    0.0     0.020900.052100.012800.00593
3.-4.    0.0     0.0     0.016400.025500.00360
4.-6.    0.0     0.0     0.0     0.011400.01290
6.-8.    0.0     0.0     0.0     0.0     0.00281
   0.96208E 05
 *** 12/20/71-8  9" CONCRETE ALBEDO  ALPHA=51.8 BETA=87.6 GAMMA=37.8 ***
  1     0.800E 06     0.861E 04
  2     0.900E 06     0.857E 04
  3     0.100E 07     0.700E 04
  4     0.110E 07     0.541E 04
  5     0.120E 07     0.460E 04
  6     0.130E 07     0.430E 04
  7     0.140E 07     0.409E 04
  8     0.150E 07     0.374E 04
  9     0.160E 07     0.326E 04
 10     0.170E 07     0.276E 04
 11     0.180E 07     0.231E 04
 12     0.190E 07     0.198E 04
 13     0.200E 07     0.181E 04
 14     0.210E 07     0.181E 04
 15     0.220E 07     0.189E 04
 16     0.230E 07     0.198E 04
 17     0.240E 07     0.200E 04
 18     0.250E 07     0.194E 04
 19     0.260E 07     0.176E 04
 20     0.270E 07     0.152E 04
 21     0.280E 07     0.127E 04
 22     0.290E 07     0.105E 04
 23     0.300E 07     0.873E 03
 24     0.320E 07     0.632E 03
 25     0.340E 07     0.488E 03
 26     0.360E 07     0.438E 03
 27     0.380E 07     0.411E 03
 28     0.400E 07     0.344E 03
 29     0.420E 07     0.264E 03
 30     0.440E 07     0.205E 03
 31     0.460E 07     0.165E 03
 32     0.480E 07     0.133E 03
 33     0.500E 07     0.107E 03
 34     0.520E 07     0.857E 02
 35     0.540E 07     0.700E 02
 36     0.560E 07     0.601E 02
 37     0.580E 07     0.517E 02
 38     0.600E 07     0.408E 02
 39     0.620E 07     0.297E 02
 40     0.640E 07     0.218E 02
 41     0.660E 07     0.170E 02
 42     0.680E 07     0.150E 02
 43     0.700E 07     0.142E 02
 44     0.720E 07     0.120E 02
 45     0.740E 07     0.818E 01
 46     0.760E 07     0.510E 01
```

47	0.780E 07	0.348E 01
48	0.800E 07	0.264E 01
49	0.820E 07	0.244E 01
50	0.840E 07	0.301E 01
51	0.860E 07	0.377E 01
52	0.880E 07	0.415E 01
53	0.900E 07	0.415E 01
54	0.920E 07	0.385E 01
55	0.940E 07	0.312E 01
56	0.960E 07	0.197E 01
57	0.980E 07	0.630E 00
58	0.100E 08	-0.651E 00
59	0.102E 08	-0.175E 01
60	0.104E 08	-0.246E 01
61	0.106E 08	-0.256E 01
62	0.108E 08	-0.204E 01
63	0.110E 08	-0.122E 01
64	0.112E 08	-0.405E 00
65	0.114E 08	0.231E 00
66	0.116E 08	0.655E 00
67	0.118E 08	0.823E 00
68	0.120E 08	0.794E 00
69	0.122E 08	0.728E 00
70	0.124E 08	0.791E 00
71	0.126E 08	0.100E 01
72	0.128E 08	0.124E 01
73	0.130E 08	0.134E 01
74	0.132E 08	0.130E 01
75	0.134E 08	0.120E 01
76	0.136E 08	0.115E 01
77	0.138E 08	0.113E 01
78	0.140E 08	0.109E 01
79	0.142E 08	0.999E 00
80	0.144E 08	0.884E 00
81	0.146E 08	0.827E 00
82	0.148E 08	0.880E 00
83	0.150E 08	0.104E 01
84	0.152E 08	0.129E 01
85	0.154E 08	0.159E 01
86	0.156E 08	0.193E 01
87	0.158E 08	0.226E 01
88	0.160E 08	0.249E 01
89	0.162E 08	0.254E 01
90	0.164E 08	0.240E 01
91	0.166E 08	0.208E 01
92	0.168E 08	0.166E 01
93	0.170E 08	0.123E 01
94	0.172E 08	0.847E 00
95	0.174E 08	0.546E 00
96	0.176E 08	0.330E 00
97	0.178E 08	0.189E 00
98	0.180E 08	0.102E 00

99	0.182E 08	0.529E-01
100	0.184E 08	0.262E-01
101	0.186E 08	0.124E-01
102	0.188E 08	0.567E-02
103	0.190E 08	0.250E-02
104	0.192E 08	0.107E-02
105	0.194E 08	0.445E-03

ALBEE Output

```
*** CRNL ALBEDO VALUES   THETAG=63 , THETA=128 , PHI=135 ***
      1       0.438E-01
      2       0.278E-01
      3       0.186E-01
      4       0.179E-01
      5       0.646E-02
      6       0.242E-02
      7       0.152E-03
*** 12/20/71-8  9" CONCRETE ALBEDO  ALPHA=51.8 BETA=87.6 GAMMA=37.8 ***
      1       0.289E-01
      2       0.314E-01
      3       0.289E-01
      4       0.219E-01
      5       0.193E-01
      6       0.193E-01
      7       0.182E-01
      8       0.172E-01
      9       0.154E-01
     10       0.134E-01
     11       0.117E-01
     12       0.102E-01
     13       0.927E-02
     14       0.987E-02
     15       0.106E-01
     16       0.107E-01
     17       0.106E-01
     18       0.109E-01
     19       0.100E-01
     20       0.872E-02
     21       0.747E-02
     22       0.637E-02
     23       0.526E-02
     24       0.426E-02
     25       0.336E-02
     26       0.314E-02
     27       0.312E-02
     28       0.243E-02
     29       0.192E-02
     30       0.158E-02
     31       0.121E-02
     32       0.984E-03
     33       0.817E-03
     34       0.634E-03
     35       0.521E-03
     36       0.456E-03
     37       0.395E-03
     38       0.313E-03
     39       0.231E-03
     40       0.170E-03
     41       0.131E-03
     42       0.116E-03
     43       0.109E-03
     44       0.939E-04
     45       0.660E-04
     46       0.423E-04
     47       0.290E-04
     48       0.214E-04
```

MEASURED FAST-NEUTRON ALBEDOS FOR CONCRETE AND STEEL: COMPARISON WITH CALCULATIONS

by

JOHN WAYNE LEIGHTY

B.S., Kansas State University, 1970

AN ABSTRACT OF A MASTER'S THESIS

submitted in partial fulfillment of the

requirements for the degree

MASTER OF SCIENCE

Department of Nuclear Engineering

KANSAS STATE UNIVERSITY
Manhattan, Kansas

1972

ABSTRACT

Fast-neutron albedos were experimentally determined for a 24 x 24 x 9 inch thick concrete slab and a 24 x 24 x 6 inch thick cold roll steel slab. The experimental dose albedos were compared with Oak Ridge National Laboratory 05R Monte Carlo calculated dose albedos. Orders-of-scattering calculations were also performed to generate reflected spectra for comparison with the experimental albedo results.

The source of fast-neutrons for the experimental studies was the KSU Triga Mark II reactor; the direct and reflected neutron spectra were detected using a 2 x 2 inch NE-213 liquid scintillation spectrometer system. A computer code has been developed to normalize the experimental reflected spectra to a reference direct neutron beam measurement, to calculate the experimental dose albedos, and to evaluate the Monte Carlo dose albedos in terms of the experimental conditions. A comparison of the Monte Carlo and experimental results showed similar trends and structure but the experimental dose albedos were smaller than the Monte Carlo calculated albedos by an average of 70 to 80%. The energy bin widths used in the Monte Carlo calculations were 1 to 2 MeV in width which would tend to increase the value of the calculated dose albedos. In addition the cross sections used in the Monte Carlo calculations have subsequently been found to be in error by as much as 65%.

Orders-of-scattering calculations for steel were performed using the ORNL DLC-2B 99 group cross section set and similar calculations were performed for concrete using the DLC-9 122 group cross section set. The orders-of-scattering calculated steel reflected spectra compare well with the experimental fast-neutron reflection spectra. Various discrepancies were noted in concrete spectra calculated with DLC-9 multigroup cross sections

and thus comparisons of the orders-of-scattering and experimental results for concrete were not possible.